

# Split Dirac supersymmetry: An ultraviolet completion of Higgsino dark matter

Patrick J. Fox,<sup>1</sup> Graham D. Kribs,<sup>2,3</sup> and Adam Martin<sup>4</sup><sup>1</sup>*Theoretical Physics Department, Fermilab, P.O. Box 500, Batavia, Illinois 60510, USA*<sup>2</sup>*School of Natural Sciences, Institute for Advanced Study, Princeton, New Jersey 08540, USA*<sup>3</sup>*Department of Physics, University of Oregon, Eugene, Oregon 97403, USA*<sup>4</sup>*Department of Physics, University of Notre Dame, Notre Dame, Indiana 46556, USA*

(Received 22 May 2014; published 7 October 2014)

Motivated by the observation that the Higgs quartic coupling runs to zero at an intermediate scale, we propose a new framework for models of split supersymmetry, in which gauginos acquire intermediate scale Dirac masses of  $\sim 10^{8-11}$  GeV. Scalar masses arise from one-loop finite contributions as well as direct gravity-mediated contributions. Like split supersymmetry, one Higgs doublet is fine-tuned to be light. The scale at which the Dirac gauginos are introduced to make the Higgs quartic zero is the same as is necessary for gauge coupling unification. Thus, gauge coupling unification persists (nontrivially, due to adjoint multiplets), though with a somewhat higher unification scale  $\gtrsim 10^{17}$  GeV. The  $\mu$  term is naturally at the weak scale, and provides an opportunity for experimental verification. We present two manifestations of split Dirac supersymmetry. In the “pure Dirac” model, the lightest Higgsino must decay through  $R$ -parity violating couplings, leading to an array of interesting signals in colliders. In the “hypercharge impure” model, the bino acquires a Majorana mass that is one-loop suppressed compared with the Dirac gluino and wino. This leads to weak scale Higgsino dark matter whose overall mass scale, as well as the mass splitting between the neutral components, is naturally generated from the same UV dynamics. We outline the challenges to discovering pseudo-Dirac Higgsino dark matter in collider and dark matter detection experiments.

DOI: 10.1103/PhysRevD.90.075006

PACS numbers: 14.80.Da, 12.60.Jv

## I. INTRODUCTION

In the minimal supersymmetric extension of the Standard Model (MSSM), the Higgs quartic coupling is predicted, in terms of a handful of parameters that determine the tree-level and loop-corrected contributions. Now that the LHC has measured the Higgs mass [1,2], and consequently the quartic coupling in the Standard Model, this measurement can be used to reverse-engineer the parameters and relevant mass scales of the supersymmetric theory. Scales well above the weak scale are predicted:  $m_{\tilde{t}} \approx 5$  TeV for  $\tan\beta \gg 1$  and  $|A_t| \ll m_{\tilde{t}}$  (e.g. [3–7]) and in split supersymmetry [8–10]  $m_{\tilde{t}} \gtrsim 10^8$  GeV for  $\tan\beta \approx 1$  [11–14]. The long tail to very large superpartner masses results from the vanishing of the tree-level quartic coupling in the  $\tan\beta \rightarrow 1$  limit. Reverse-engineering the mass scales of the MSSM is unfortunately not very predictive after all.

Supersymmetric models with Dirac gaugino masses, first studied in [15–17] with more model-building explored in [18–37], predict the Higgs quartic coupling to vanish once the gauginos and their scalar counterparts are integrated out<sup>1</sup> [18]. This is an improvement on the MSSM, in so far as there is a single prediction for the scale of supersymmetry breaking masses. Reverse-engineering this scale, and

one finds  $M_D \sim 10^{11}$  GeV, where  $\lambda_h(M_D) \approx 0$  (for example, [38–45]). This is akin to the original split supersymmetry models [8–10], except that both gauginos and scalars are expected to be within an order of magnitude of this large intermediate scale. Unlike split supersymmetry models, however, there are negligible corrections to the running of the Standard Model quartic coupling for scales below  $\ll M_D$  (and hence the difference between the upper bound of  $\sim 10^8$  GeV in split supersymmetry models with light gauginos [11] from  $\sim 10^{11}$  GeV in split Dirac supersymmetry models). Other recent versions of intermediate scale supersymmetry include [46–53].

This is an idealized scenario. In practice, there are additional contributions to the Higgs quartic coupling even in models with dominantly Dirac gaugino masses. For one, anomaly mediation provides an irreducible Majorana contribution to gaugino masses as well as a separate contribution to the adjoint scalar masses, the latter causing corrections to the pure Dirac prediction of a vanishing quartic coupling. The size of Majorana masses is naturally loop-suppressed compared with the Dirac gaugino masses, for example in models with gravity mediation [30]. This leads to a very small contribution to the quartic coupling. Another contribution arises from the dimension-six (so called “lemon-twist”) operator [18] in the superpotential,  $W'W'\text{tr}\Phi^2/M^2$ , that results in shifts of the masses of scalar components of the adjoint superfields. The mass shifts

<sup>1</sup>Assuming just the dimension-five supersoft operator; more on this in Sec. II.

cause an incomplete cancellation of the quartic, though it is controllable within the order one differences between the coefficients of these operators and  $\tan\beta$ . Yet another contribution is a supersymmetric mass for the adjoint superfield, which shifts both the gaugino masses as well as the scalar masses, the latter causing corrections to the pure Dirac prediction of a vanishing quartic coupling as before. Finally, the superpotential operator that generates Dirac gaugino masses may not exist for all of the gauge groups. In the hypercharge impure model that we discuss below, there is no singlet partner for the bino, and thus, the bino does not acquire a Dirac mass. As a consequence, the bino acquires a loop-suppressed Majorana mass from anomaly mediation, and regenerates a small Higgs quartic coupling,  $\lambda_h \approx (g^2 \cos^2 2\beta)/4$ . This implies a restricted range of intermediate scales for the supersymmetry breaking masses is predicted, between  $10^8$  to  $10^{10}$  GeV, corresponding to between  $\tan\beta \gg 1$  to  $\tan\beta \approx 1$ .

The  $\mu$  parameter could be small or near the intermediate scale, depending on whether a “bare”  $U(1)_{PQ}$ -breaking mass,  $\int d^4\theta H_u H_d$ , is permitted [13]. As a chiral Kähler operator, it is technically natural to omit it, which we do. Thus, we consider  $B_\mu$  and  $\mu$  generated through higher-dimensional operators after supersymmetry is broken. Kähler operators at dimension six can lead to both  $B_\mu$  and  $\mu$  from  $D$ -term and  $F$ -term contributions. If there are no singlets in the hidden sector, which is consistent with the gauginos not acquiring Majorana masses (except through anomaly mediation), the leading operator to generate  $\mu$  is  $\int d^4\theta W'^{\dagger} W'^{\dagger} H_u H_d / \Lambda^3$ , which is dimension seven, and thus suppressed relative to the intermediate scale.  $B_\mu$  can arise through a dimension-six operator in the superpotential  $\int d^2\theta W' W' H_u H_d / \Lambda^2$ , whose coefficient is set by doing one fine-tuning to get one Higgs doublet light. Given  $B_\mu$ , as well as anomaly-mediated Majorana contributions to the gaugino masses, both  $U(1)_{PQ}$  and  $U(1)_R$  are broken in the visible sector near the intermediate scale, and thus there is also a one-loop radiative contribution to  $\mu$  [9,10]. In the hypercharge impure model, this one-loop radiative contribution provides the dominant contribution to  $\mu$ , analogous to one version of spread supersymmetry [12], as we will see.

Remarkably, gauge coupling unification persists when  $\mu \sim$  weak scale with a Dirac gluino and Dirac wino at an intermediate scale. Gauge coupling unification with intermediate scale Dirac gauginos has been studied before [22], and unification occurs with fairly good accuracy even when light Higgsinos are the only new physics affecting gauge coupling running [54,55]. In the models we consider, given a weak scale  $\mu$  parameter, the leading difference at one-loop from the MSSM is the *scale* of the Dirac gaugino masses and the additional *degrees of freedom* due to the additional adjoint chiral superfields. Since the degrees of freedom are proportional to the appropriate quadratic Casimir of the group [ $N$  for  $SU(N)$ ], there is some common Dirac gaugino

mass scale where gauge coupling unification *must occur*. Remarkably, we find  $M_D \approx 10^{11}$  GeV, which is essentially the same scale where  $\lambda_h(M_D) \approx 0$ . The additional degrees of freedom (Dirac fermion partner and complex scalar in the adjoint representation) accelerate the RG evolution of the gauge couplings between the intermediate scale to the unification scale in such a way as to exactly compensate for the lack of Majorana gauginos in the RG evolution between the weak scale and the intermediate scale. This is discussed in Sec. III.

The outline of the paper is as follows. We first present the “toolkit” for split Dirac supersymmetry models in Sec. II. This includes the variety of operators and contributions to the soft masses and  $\mu$  parameter in the theory. We demonstrate gauge coupling unification is successful at one loop in Sec. III. Gauge coupling unification, however, is not directly affected by the character of the bino, i.e., whether there is (or is not) a pure singlet superfield for it to acquire a Dirac mass. This leads to two distinct models within the larger framework of split Dirac supersymmetry:

- (i) Pure Dirac model (Sec. IV): The gluino, wino, and bino acquire Dirac masses. In this model, the Higgs quartic coupling vanishes at the intermediate scale, and thus predicts the largest scale for the Dirac gauginos. The Higgsino mass is small, arising from a dimension-seven operator as well as a suppressed radiative contribution. The neutral Higgsinos are highly degenerate,  $\Delta m_\chi \ll$  keV, forming a nearly pure Dirac fermion with an unsuppressed  $Z$  coupling, and are ruled out as a dark matter candidate.  $R$ -parity violation is introduced, and we demonstrate the various decay modes that are possible for the lightest Higgsino.
- (ii) Hypercharge impure model (Sec. V): The gluino and wino acquire Dirac masses, while the bino acquires a

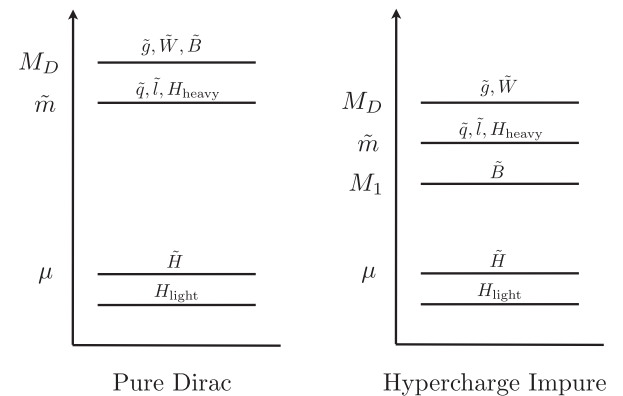


FIG. 1. Sketch of the mass spectrum of the two split Dirac supersymmetry models considered in this paper: Pure Dirac (all gauginos acquire Dirac masses) and hypercharge impure (the gluino and wino acquire Dirac masses, the bino acquires a Majorana mass).

Majorana mass from anomaly mediation, making it lighter than the other gauginos. In this scenario, a small quartic coupling may be regenerated, depending on  $\tan\beta$  (which in turn depends on the relative hierarchy between  $B_\mu$  and  $m_{H_u}^2, m_{H_d}^2$ ). Generally, a slightly lower scale for  $M_D \sim 10^8 \rightarrow 10^9$  GeV results, causing  $M_1 \sim 10^6 \rightarrow 10^7$  GeV. This large bino mass has the feature of generating the scale of  $\mu$  and the mass splitting  $m_{\tilde{\chi}_2} - m_{\tilde{\chi}_1} \simeq M_Z^2 \sin^2 \theta_W / M_1$  to make the lightest Higgsino a perfect WIMP candidate for dark matter.

The mass spectra associated with each of these models is shown in Fig. 1. Finally, we conclude with a discussion in Sec. VI.

## II. TOOLKIT FOR SPLIT DIRAC SUPERSYMMETRIC MODELS

Split Dirac supersymmetry is a general framework for considering a new class of split supersymmetry models. In this section, we provide an overview of the operators leading to contributions to the supersymmetry breaking and preserving parameters in the (Dirac extended) MSSM. This serves as a ‘‘toolkit’’ with which split Dirac supersymmetry model enthusiasts can build interesting models. We use the results of the toolkit to construct the two models that serve as the focus of this paper in Secs. IV and V.

### A. No singlets in the hidden sector

Majorana gaugino masses arise when total gauge singlets in the hidden sector,  $S$ , acquire supersymmetry breaking vevs for their  $F$  components,  $S = F\theta^2$ . The usual dimension-five operator that leads to Majorana gauginos is  $\int d^2\theta SW_\alpha W^\alpha / \Lambda$ . While it is always technically natural to omit these contributions, if there no singlets in the hidden sector, this operator is simply forbidden. In addition, the absence of hidden sector singlets also means the usual dimension-five operator in the Kähler potential that generates  $\mu$ ,  $\int d^4\theta S^\dagger H_u H_d / \Lambda$ , is forbidden. Hidden sectors without singlets are well known, for example  $SU(4) \times U(1)$  [56]. In the absence of hidden sector singlets, gauginos can acquire Dirac masses through  $D$ -type expectation values, as explained below, as well as anomaly-mediated Majorana masses. The  $\mu$  term can arise through higher-dimensional operators, or through radiative corrections, as we will see.

### B. Dirac gaugino masses

A Dirac gaugino mass for one or more gauge groups of the Standard Model arises once the MSSM is extended with an additional superfield  $\Phi_k$  in the adjoint representation of the appropriate gauge group,  $k = 1, 2, 3$  for  $U(1)_Y, SU(2)_L, SU(3)_c$ . The Dirac mass is generated through the operator

$$\mathcal{L} \supset \lambda_k \int d^2\theta \sqrt{2} \frac{\mathbf{W}'_a \mathcal{W}_a^{k,\alpha} \Phi_{k,a}}{\Lambda} + \text{H.c.}, \quad (1)$$

where  $\mathbf{W}'_a = \theta_a \mathbf{D}$  is a spurion for supersymmetry breaking,  $\mathcal{W}_a^{k,\alpha}$  is the gauge superfield for the appropriate SM gauge group, and  $\Lambda$  is the scale where supersymmetry breaking is mediated to the visible sector. The labels  $\alpha$  and  $a$  are spinor and gauge indices, respectively. Inserting the  $D$ -term expectation value, the operator gives

$$\mathcal{L} \supset -M_{D,k} (\lambda_a \psi_a + 2\sqrt{2} D_a \text{Re}(A_a)) + \text{H.c.}, \quad (2)$$

where  $A_a$  is the complex scalar of the supermultiplet  $\Phi_a$ . This term marries the gaugino  $\lambda_a$  with a fermion in the adjoint representation  $\psi_a$  with a Dirac mass  $M_{D,k} \equiv \lambda_k \mathbf{D} / \Lambda$ .

### C. Higgs quartic coupling at dimension five

The tree-level quartic coupling for Higgs boson arises from the  $D$  terms. The new ingredient from the dimension-five operator of Eq. (2), is the term  $2\sqrt{2} M_D D_a \text{Re}(A_a)$  in addition to the term  $-D_a^2/2$  from the gauge kinetic terms in the superpotential. Solving for the  $D$  term through its equation of motion gives

$$D_a = -2\sqrt{2} M_D \text{Re}(A_a) + g_a^2 \sum_i \phi_i^* t^a \phi_i. \quad (3)$$

Substituting this back into Lagrangian,

$$\frac{1}{2} \left( 2\sqrt{2} M_D \text{Re}(A_a) + g_a^2 \sum_i \phi_i^* t^a \phi_i \right)^2, \quad (4)$$

we find the usual Higgs quartic coupling, a mass for  $\text{Re}(A_a)$ , and a cross term. Once  $\text{Re}(A_a)$  is integrated out at  $\simeq M_D$ , no quartic couplings proportional to gauge couplings remain. Hence, the tree-level Higgs quartic coupling vanishes.

### D. Higgs quartic coupling at dimension six

There are additional contributions to the quartic coupling. Using just  $D$  terms, at dimension six one can write the lemon-twist operator

$$\frac{\lambda_{\text{lt}}}{2} \int d^2\theta \frac{\mathbf{W}'_a \mathbf{W}'^a}{\Lambda^2} \text{tr}(\Phi_a \Phi_a) + \text{H.c.} \quad (5)$$

This superpotential term gives masses to both  $\text{Re}(A_a)$  and  $\text{Im}(A_a)$  scalar components of  $\Phi_a$ , but with opposite sign. This additional mass term for  $\text{Re}(A_a)$  disrupts the quadratic form, Eq. (4), and thus can reintroduce a partial quartic coupling for the Higgs boson. The size of the quartic depends on the relative size of the operator coefficients,<sup>2</sup>

<sup>2</sup>Throughout this paper, we use the normalization convention  $V(H) \supset \frac{\lambda_H}{2} (H^\dagger H)^2$  for the Higgs quartic.

$$\Delta\lambda_{h,\text{tree}} = \frac{1}{4} \cos^2 2\beta \left( \frac{\lambda_h g^2}{4\lambda_2^2 + \lambda_{\text{it}}} + \frac{\lambda_h g^2}{4\lambda_1^2 + \lambda_{\text{it}}} \right). \quad (6)$$

In many UV completions this operator is generated at the same order as the operator of Eq. (1), and thus is too large. However, solutions to this problem have been proposed [57]. It should also be noted that it is technically natural to omit this contribution from the superpotential, so its absence need not require tuning coefficients. It is also true that a modest hierarchy between the dimension-five coefficient and the dimension-six coefficient will also render this contribution to the quartic coupling to be negligible.

### E. Majorana gaugino masses

In the absence of singlets in the hidden sector, Majorana gaugino masses arise from anomaly mediation. Placed in the context of supergravity and tuning away the cosmological constant, supersymmetry breaking generates a gravitino mass at least of order

$$m_{3/2} \sim \frac{\mathbf{D}}{\sqrt{3}M_{\text{pl}}}. \quad (7)$$

(Here we assume the  $D$  term dominates the supersymmetry breaking in the hidden sector.) The anomaly-mediated contribution to the Majorana gaugino masses is [58,59]

$$\tilde{M}_k = \frac{\beta_k}{g_k} m_{3/2}, \quad (8)$$

where  $\beta_k$  are the gauge coupling beta-functions given in Appendix B. Comparing the size of the Dirac and Majorana gaugino masses, we find

$$\frac{\tilde{M}_k}{M_{D,k}} = \frac{\beta_k}{g_k \lambda_k} \frac{\Lambda}{M_{\text{pl}}}. \quad (9)$$

We see that the Majorana gaugino masses are suppressed by at least a loop factor times gauge coupling squared relative to the Dirac gaugino masses. Further suppression is possible if the mediation scale is below the Planck scale. The Majorana mass splits the Dirac gaugino state into two Majorana states—though the loop suppression from Eq. (9) implies that the splitting between the states is small and the gauginos are more accurately described as pseudo-Dirac. Pseudo-Dirac gauginos do not in themselves change the argument about the vanishing of the quartic coupling. In anomaly mediation, the gaugino masses are also accompanied by scalar mass squareds that are two-loop suppressed relative to the gravitino mass, but this leads to a very small correction for the Majorana masses given in Eq. (9).

### F. Higgs quartic coupling with supersymmetric masses for the adjoints

Supersymmetric masses for the adjoint fields can be generated through the operator

$$\frac{\lambda_{\text{adj}}}{2} \int d^4\theta \left( \frac{\mathbf{W}'^\dagger_\alpha \mathbf{W}'^{\alpha\dagger}}{\Lambda^3} \text{tr}(\Phi_a \Phi_a) + \text{H.c.} \right), \quad (10)$$

which gives a very small supersymmetric contribution to the masses of the adjoint fields,  $M_{\text{adj}} \equiv \lambda_{\text{adj}} \mathbf{D}^2 / \Lambda^3$ . In principle this contribution modifies the quartic coupling [18]

$$\Delta\lambda_{h,\text{tree}} = \frac{1}{4} \cos^2 2\beta \left( \frac{g^2 M_{\text{adj},2}^2}{M_{\text{adj},2}^2 + 4M_{D,2}^2} + \frac{g'^2 M_{\text{adj},1}^2}{M_{\text{adj},1}^2 + 4M_{D,1}^2} \right). \quad (11)$$

Given that  $M_{\text{adj}} \sim M_D^2 / \Lambda$ , this leads to a negligible correction. If however “bare” supersymmetric masses for the adjoints were present in the superpotential,  $\mathcal{O}(1) \int d^2\theta M_{\text{adj}} \text{tr}(\Phi_a \Phi_a) + \text{H.c.}$ , independent of supersymmetry breaking, with masses of order or exceeding the Dirac masses, then a partial quartic is recovered. For example, in the hypercharge impure model detailed in Sec. V, the bino does not acquire a Dirac mass. This could occur even with the existence of Eq. (1) with a bino superfield partner (a total gauge singlet), if the mass  $M_{\text{adj},1} \gg M_{D,1}$ , so that  $\lambda_h = g'^2 \cos^2 2\beta / 4$  from Eq. (11).

### G. $\mu$ and $B_\mu$ term from $D$ terms

Using just  $D$ -type spurions, both  $U(1)_{PQ}$  and  $U(1)_R$  can be violated through higher-dimensional operators. As a result, both  $\mu$  and  $B_\mu$  can be generated. The leading contribution to  $\mu$  is from

$$\begin{aligned} \int d^4\theta \frac{\mathbf{W}'^\dagger_\alpha \mathbf{W}'^{\alpha\dagger} H_u H_d}{\Lambda^3} &= \int d^2\theta \frac{D^2}{\Lambda^3} H_u H_d \\ &= \int d^2\theta \frac{M_D^2}{\Lambda} H_u H_d \end{aligned} \quad (12)$$

that gives  $\mu \sim \text{TeV}$  when  $M_D \sim 10^{11}$  GeV and  $\Lambda = M_{\text{pl}}$ . Notice also that once  $M_D \lesssim 10^{10}$  GeV (for  $\Lambda = M_{\text{pl}}$ ), this contribution becomes too small to give a large enough  $\mu$  to evade direct collider constraints on Higgsinos. We will refer to this  $\mu$ -term contribution as the “primordial”  $\mu$ .

The leading contribution to  $B_\mu$  arises from the superpotential operator

$$\lambda_{B_\mu} \int d^2\theta \frac{\mathbf{W}'_\alpha \mathbf{W}'^{\alpha} H_u H_d}{\Lambda^2} = \lambda_{B_\mu} \frac{D^2}{\Lambda^2} \tilde{H}_u \tilde{H}_d. \quad (13)$$

Notice that  $B_\mu$  is parametrically of the same size as the Dirac gaugino mass found in Eq. (2).



## H. Radiative generation of $\mu$

The global symmetries  $U(1)_{PQ}$  and  $U(1)_R$  are broken by the  $B_\mu$  term and Majorana gaugino masses. In a model *without* Dirac mass terms for the bino and wino, this implies  $\mu$  can be radiatively generated [10] through the renormalization group equation,<sup>3</sup>

$$(4\pi)^2 \frac{d\mu}{dt} = \tilde{g}'_u \tilde{g}'_d M_1^* + 3\tilde{g}_u \tilde{g}_d M_2^* + \frac{1}{4}\mu \left[ -18 \left( \frac{g_1^2}{5} + g_2^2 \right) + 3(\tilde{g}_u^2 + \tilde{g}_d^2) + \tilde{g}'_u{}^2 + \tilde{g}'_d{}^2 \right]. \quad (14)$$

The  $\tilde{g}'_{u,d}(\tilde{g}_{u,d})$  couplings are the strengths of the up or down-type Higgsino-Higgs-bino (Higgsino-Higgs-wino) Yukawa couplings. At the scale of supersymmetry breaking  $M_D$ , these Yukawa couplings are related, at tree level, to the gauge couplings as  $\tilde{g}'_u(M_D) = g' \sin \beta$ ,  $\tilde{g}'_d(M_D) = g' \cos \beta$ , etc. However, below  $M_D$ , the theory is no longer supersymmetric so the RGE for the Higgsino-Higgs-bino Yukawa couplings is no longer the same as the RGE for the gauge couplings. The RGE for  $\mu$  is proportional to  $\sin(2\beta)$ , which vanishes in the limit  $\tan \beta \rightarrow \infty$  (or 0). This follows because, in this limit,  $B_\mu \propto \sin(2\beta) \rightarrow 0$ , and hence  $U(1)_{PQ}$  symmetry is restored [10].

If however both the bino and wino acquire Dirac masses, the only source of  $U(1)_R$  breaking is the small anomaly-mediated Majorana gaugino mass. Therefore, the RGE in Eq. (14) only applies between the two narrowly split pseudo-Dirac states (between  $M_{D,1} \pm \tilde{M}_1$ ). As a result, the radiatively generated  $\mu$  is highly suppressed. We will see examples of both  $M_{D,k} = 0$  and  $M_{D,k} \neq 0$  in the models discussed in Secs. V, IV.

## I. One-loop finite contributions to scalar masses

Supersymmetry breaking through  $D$  terms is known as supersoft supersymmetry breaking [18] due to the finite soft scalar (mass)<sup>2</sup> that are induced for the scalars of the MSSM. The contributions were computed in [18] to be

$$\tilde{m}^2 = \sum_k \frac{C_k(r) \alpha_k M_{D,k}^2}{\pi} \log \frac{\tilde{m}_{r,k}^2}{M_{D,k}^2}. \quad (15)$$

Here  $\tilde{m}_{r,k}$  is the scalar mass for the real part of the adjoint field, given by  $2M_{D,k}$  in the absence of additional contributions from  $F$  terms to the scalar masses (see next subsection).

<sup>3</sup>This result includes one minor correction to the RGE for  $\mu$  given in Ref. [10]. The correct expression involves the *complex conjugate* of the gaugino mass, such that the reparameterization-invariant phases  $\arg(\tilde{g}'_u{}^* \tilde{g}'_d{}^* \mu M_1)$  and  $\arg(\tilde{g}'_u \tilde{g}'_d{}^* \mu M_2)$  are not generated if there is no primordial contribution to  $\mu$ .

## J. $F$ -term contributions to scalar masses

Supersymmetry breaking hidden sectors with  $D$ -term spurions (which was utilized above to generate the Dirac gaugino mass) generically have spurions,  $\mathbf{X}$ , that transform under the hidden sector group (i.e. non-singlets), and acquire  $F$  terms (e.g., see [56]). The only gauge invariant combination of the hidden sector spurions  $\mathbf{X}$  that get  $F$ -type expectation values must involve powers of  $\mathbf{X}^\dagger \mathbf{X}$ . This implies mass terms for scalars

$$\kappa_i \int d^4\theta \frac{\mathbf{X}^\dagger \mathbf{X}}{\Lambda^2} \phi_i^\dagger \phi_i, \quad (16)$$

as well as a contribution the  $B_\mu$  term,

$$\kappa_{B_\mu} \int d^4\theta \frac{\mathbf{X}^\dagger \mathbf{X}}{\Lambda^2} H_u H_d, \quad (17)$$

are generically present. These operators give contributions  $|F|^2/\Lambda^2$  to the scalar mass squareds as well as  $B_\mu$ .

## K. Fine-tuning to get one light Higgs doublet

In split supersymmetry models, fine-tuning in the scalar mass squared parameters of the Higgs mass matrix is needed such that one doublet gets a small, negative mass squared, causing electroweak symmetry breaking [8–10] (see also [12,13,60,61]). In the MSSM, the Higgs mass matrix is

$$\mathcal{M}_H = \begin{pmatrix} m_{H_u}^2 & B_\mu \\ B_\mu & m_{H_d}^2 \end{pmatrix}, \quad (18)$$

where the entries in the mass matrix include all of the supersymmetry breaking contributions from  $D$  terms and  $F$  terms described above. (We have neglected the tiny contribution  $|\mu|^2 \ll |m_{H_u}^2|, |m_{H_d}^2|$  to the diagonal entries.) Since the Dirac gauginos induce large positive one-loop finite contributions to  $m_{H_u}^2$  and  $m_{H_d}^2$ , we assume any additional contributions from  $F$  terms do not cause these mass-squareds to go negative. Electroweak symmetry breaking at the weak scale requires one small negative eigenvalue, and hence  $\text{Det}[\mathcal{M}_H] = m_{H_u}^2 m_{H_d}^2 - B_\mu^2 < 0$ . The light (negative) eigenvalue is

$$\begin{aligned} m_{H_{\text{light}}}^2 &\simeq \frac{\text{Det}[\mathcal{M}_H]}{\text{Tr}[\mathcal{M}_H]} = \frac{m_{H_u}^2 m_{H_d}^2 - B_\mu^2}{m_{H_u}^2 + m_{H_d}^2} \\ &= \frac{1}{1 + \tan^2 \beta} \left[ m_{H_u}^2 \tan^2 \beta - \frac{B_\mu^2}{m_{H_u}^2} \right], \end{aligned} \quad (19)$$

where  $\tan \beta$  is determined by

$$\tan \beta \simeq \sqrt{\frac{m_{H_d}^2}{m_{H_u}^2}}, \quad (20)$$

up to corrections of order  $m_{H_{\text{light}}}^2/(m_{H_u}m_{H_d})$ . Clearly we must fine-tune  $B_\mu^2$  to be slightly larger than  $m_{H_u}^2 m_{H_d}^2$  to obtain a small negative mass-squared eigenvalue.

It is interesting to compare the size of  $B_\mu$  to the one-loop (finite) contributions from the Dirac gauginos to the Higgs soft mass squared(s). The largest contributions to the soft mass squareds for the Higgs doublets come from the Dirac wino,

$$m_{H_u}^2 \approx m_{H_d}^2 \approx \frac{g^2}{4\pi^2} M_{D,2}^2 \approx \left(\frac{M_{D,2}}{10}\right)^2. \quad (21)$$

Comparing this to the size of  $B_\mu$  given in Eq. (13), we need  $\lambda_{B_\mu} \approx 10^{-2}$  such that  $B_\mu$  marginally destabilizes the Higgs mass matrix giving one negative eigenvalue. Since this contribution to  $B_\mu$  arises in the superpotential, it is technically natural for this coefficient to be small.

Notice also that when the one-loop finite contributions from the Dirac gauginos dominate the Higgs mass squareds, Eq. (21),  $m_{H_u}^2 \approx m_{H_d}^2$  and thus  $\tan\beta \approx 1$ . Once  $F$ -term contributions are included with different coefficients for the up-type and down-type masses,  $\tan\beta$  can be different from 1. Generically, in the absence of large hierarchies in these coefficients,  $\tan\beta$  is small.

### III. GAUGE COUPLING UNIFICATION AT ONE LOOP

We now discuss gauge coupling unification in split Dirac supersymmetry models. This discussion provides a common framework that illustrates the relevant contributions to the  $\beta$  functions, at one loop, and the expected scales of the superpartners. In the specific models described in Secs. IV and V, we numerically evaluate gauge coupling unification to two loops with the appropriate thresholds for the spectra in each theory.

Since the sfermions fill out complete GUT multiplets, they do not affect the differential running of the gauge couplings, and consequently the level of unification, and we will omit them from the discussion below. These effects are included in the numerical analysis carried out in later sections. Thus, there are two important contributions to the one-loop beta functions for the gauge couplings that determine the level of unification: Higgsinos (and Higgses) and gauginos. Given that  $\mu$  is small in split Dirac supersymmetry models [Eq. (12)], the only difference from MSSM running is the (lack of) gauginos and the scalar components of one Higgs doublet. Since the Higgs scalar doublet has a small contribution to the  $\beta$ -functions, here we focus on just the gauginos.

The solutions to the one-loop gauge coupling RGEs in the MSSM are

$$\alpha_{\text{unif}}^{-1}(\Lambda_{\text{unif}}) - \alpha_i^{-1}(\Lambda_{\text{weak}}) = \frac{b_i}{2\pi} \log\left(\frac{\Lambda_{\text{unif}}}{\Lambda_{\text{weak}}}\right), \quad (22)$$

where  $b_i = b_i^{\text{MSSM}} = (33/5, 1, -3)$  are the one-loop beta-function coefficients of the MSSM, where unification is achieved to within about 1%. Compare this with split Dirac supersymmetry,

$$\begin{aligned} \alpha_{\text{unif}}^{-1}(\Lambda_{\text{unif}}) - \alpha_i^{-1}(\Lambda_{\text{weak}}) \\ = \frac{b_i^{\text{Dirac}}}{2\pi} \log\left(\frac{\Lambda_{\text{unif}}}{M_D}\right) + \frac{b_i^{\text{MSSM}} - b_i^{\text{gaugino}}}{2\pi} \log\left(\frac{M_D}{\Lambda_{\text{weak}}}\right), \end{aligned} \quad (23)$$

where  $b_i^{\text{Dirac}} = b_i^{\text{MSSM}} + N_i$  and  $b_i^{\text{gaugino}} = 2N_i/3$ , with  $N_i = 0, 2, 3$  the quadratic Casimir for  $U(1)_Y$ ,  $SU(2)_L$ ,  $SU(3)_c$ . The scale for the Higgsinos is assumed to be same ( $= \Lambda_{\text{weak}}$ ) for both Eqs. (22) and (23). The additive factor,  $b_i^{\text{Dirac}}$ , corresponds to the usual gauginos as well as the fields in the chiral adjoint superfields. The RGE can be rewritten as

$$\begin{aligned} \alpha_{\text{unif}}^{-1}(\Lambda_{\text{unif}}) - \alpha_i^{-1}(\Lambda_{\text{weak}}) \\ = \frac{b_i^{\text{MSSM}}}{2\pi} \log\left(\frac{\Lambda_{\text{unif}}}{\Lambda_{\text{weak}}}\right) + N_i \frac{1}{2\pi} \log\left(\frac{\Lambda_{\text{unif}}}{M_D}\right) \\ - \frac{2}{3} N_i \frac{1}{2\pi} \log\left(\frac{M_D}{\Lambda_{\text{weak}}}\right). \end{aligned}$$

Crucially, the additive contribution above the scale  $M_D$  and the subtracted contribution below  $M_D$  are both proportional to the quadratic Casimir of the  $i^{\text{th}}$  gauge group,  $N_i$ . We can solve for the scale  $M_D$  where the last two terms cancel against each other,

$$M_D = \Lambda_{\text{unif}}^{3/5} \Lambda_{\text{weak}}^{2/5} \quad (\text{one loop}). \quad (24)$$

Notice that one obtains the same  $M_D$  for all three SM gauge groups—this occurred because the new matter that we added was in the same representation as the gauginos. Setting  $\Lambda_{\text{weak}} = \text{TeV}$ , which corresponds to a unification scale of  $2 \times 10^{16}$  GeV, we find  $M_D \sim 10^{11}$  GeV.

Having determined that the mass scale  $M_D$  necessary for Dirac supersymmetry to unify coincides with the scale where the SM Higgs quartic coupling vanishes, and that a vanishing Higgs quartic is a natural boundary condition in Dirac supersymmetry, we are ready to consider specific models. In the following sections we present two complete models within the split Dirac supersymmetry framework, each utilizing a subset of the tools presented in Sec. II. We will find that the two-loop contributions to the gauge coupling evolution cause the unification scale to increase to  $\gtrsim 10^{17}$  GeV and the precision of unification to slightly worsen, which we will quantify. (And intriguingly, this also occurs in Ref. [52].)

#### IV. PURE DIRAC MODEL

The first model we consider is one where all the gauginos acquire a Dirac mass. We construct the model from the relevant toolkit components, then consider the RG evolution in detail to self-consistently determine the mass scales in the model and the level of gauge coupling unification.

The model assumes the dominant supersymmetry breaking contributions arise from  $D$  terms, leading to the gaugino masses given in Eq. (2). In our numerical evaluations, we take the gauginos to have common mass  $M_D$ , for simplicity. The real part of the adjoint scalars,  $\text{Re}(A_a)$  also acquires a mass  $\sim M_D$ . The squarks and sleptons of the MSSM receive a (flavor-blind) supersoft contribution to their mass, Eq. (15). This mass is a threshold effect and is independent of the scale at which supersymmetry breaking is mediated. Scalar masses may also receive contributions from  $F$  terms, Eq. (16), which need not be flavor universal. The relative size of these contributions will determine the exact mass of each sfermion but, in the absence of cancellations, they are typically at least as heavy as the one-loop finite contributions from the Dirac gauginos. Anomaly mediation will also generate loop-suppressed Majorana masses for the gauginos, Eq. (9), splitting the Dirac gauginos into slightly pseudo-Dirac gauginos. There are also anomaly-mediated contributions to the scalar mass squareds (both the real and imaginary parts), though these contributions are two-loop suppressed relative to the gaugino mass squared.

In this model, there are two contributions to the  $\mu$  term. One arises from the higher-dimension operator involving  $D$  terms, Eq. (12), while the second is from the radiative generation of  $\mu$ . As discussed in Sec. II H, the radiative generation is further suppressed by the pseudo-Dirac nature of the gauginos, roughly

$$\mu_{\text{radiative}} \sim \sum_{k=1,2} \frac{g_k^2}{16\pi^2} \sin 2\beta \frac{M_{M,k}}{M_D} \frac{B_\mu}{M_D} \sim \frac{10^{-7} M_D}{\tan \beta}. \quad (25)$$

Summarizing the spectrum, the pure Dirac model contains nearly pure Dirac gauginos with mass  $M_D$ , squarks and sleptons with masses  $\tilde{m}$  (we assume  $\tilde{m} \leq M_D$ ), Higgs scalars with masses  $\tilde{m}^2 = m_{H_u} m_{H_d}$ , a  $B_\mu$  term with size  $B_\mu \approx m_{H_u} m_{H_d}$ , and  $\tan \beta = \sqrt{m_{H_u}^2 / m_{H_d}^2}$  (where  $m_{H_u}^2, m_{H_d}^2 > 0$ ). The only light states other than the Higgs boson are the Higgsinos, with mass  $\sim \text{TeV}$ . This is sketched in Fig. 1.

From Sec. III, we learned that gauge coupling unification persists when the Dirac gaugino masses are near the intermediate scale. We now carry out a more precise analysis of unification. In any given model there will be a complicated spectrum with states spread from a little above  $M_D$  to a loop factor below, with the Higgsinos at the TeV scale. Carrying out the RG evolution in such a scenario is a daunting task. However, the spreading of states over a

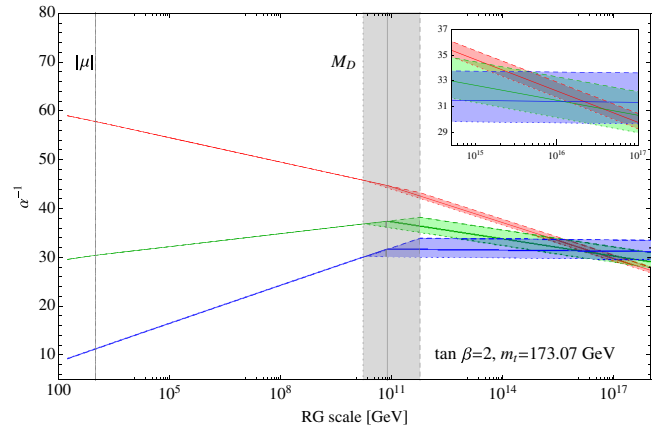


FIG. 2 (color online). An example of running for  $\mu \sim 1$  TeV and  $\tan \beta = 2$ , the scale where the Higgs quartic is zero is  $M_D = 7.5 \times 10^{10}$  GeV. The shaded regions correspond to varying  $\alpha_s(M_Z)$  within the  $2\sigma$  uncertainty.

decade or so of energy will not lead to substantially different results from the case of degeneracy. So, for simplicity, we consider a spectrum with the Higgsinos and one Higgs light, and all superpartners and the other Higgs boson heavy and degenerate, with mass  $M_D$ . At the scale  $M_D$  we match between the non-supersymmetric theory and the MSSM with additional adjoints. We carry out the running of the gauge couplings, the top Yukawa, and the Higgs self coupling, at two loops with matching at tree level. (Tree level matching implies the thresholds we discuss are not actually physical mass scales but are instead  $\overline{\text{MS}}$  masses.) We follow the approach of [44], which uses results presented in [62–66], to evolve the couplings from  $M_Z$ , given in Eq. (A2), to higher scales using the RG equations applicable to this model, given in Appendix B. The scale  $M_D$  is determined by the renormalization scale where the Higgs self-coupling passes through zero.<sup>4</sup> Under our simplifying assumptions about the spectrum there are very few parameters in this model. Once a Higgsino mass is fixed, there is a lower bound on the size of  $\tan \beta$  for this Higgsino mass to be consistent with the loop-generated contribution of Eq. (25). We show an example of the gauge coupling running in the pure Dirac model in Fig. 2. Note that the level of unification is improved as the Higgsino mass is increased.

Because of the large hierarchy between the wino/bino and the Higgsinos in this scenario, there is very little mixing among the electroweakinos, thus the two (light) neutral Majorana Higgsinos behave essentially as a single Dirac fermion. The relic abundance for a Higgsino in this mass range  $\sim \text{TeV}$ , is just right (e.g. [67]) for it to be a thermal DM relic. Unfortunately, a Dirac fermion that has quantum numbers of a neutrino has an unsuppressed elastic

<sup>4</sup>In this analysis, we assume the contribution from Eq. (6) is negligible, which is automatic if  $\tan \beta \approx 1$ .

scattering cross section off nucleons through  $Z$  exchange, and is completely ruled out by direct detection experiments.<sup>5</sup> So, the Higgsino cannot be the dark matter in this scenario, and therefore must be unstable. This can be achieved by either extending to an NMSSM-like scenario where the DM is a singlino or by adding  $R$ -parity violation to make the Higgsino decay, with DM coming from another source, e.g. an axion. We focus here on the latter possibility.

$R$ -parity violating operators fall into two classes, those that violate lepton number and those that violate baryon number. Even with squarks of mass  $\sim M_D$ , there cannot be operators with  $\mathcal{O}(1)$  coefficients from both classes since this will lead to too rapid proton decay.

For the single baryon number violating operator,  $\lambda_B u^c d^c d^c$ , the Higgsinos will decay via a virtual stop to a top and two jets. The partial width for this three-body decay is approximately

$$\Gamma_{\tilde{H}} \sim \frac{y_t^2 \lambda_B^2 \mu^5}{192 \pi^3 \tilde{m}^4}. \quad (26)$$

Yielding  $\tau_{\tilde{H}} \sim 7$  hours for TeV-scale Higgsinos,  $\lambda_B \sim 1$ , and  $\tilde{m} \sim 10^{10}$  GeV. Such long-lived Higgsinos would be completely invisible in collider detectors, but there are strong constraints on such long decays from their effects on BBN and light element abundances [69–72]. This partial width is strongly dependent on mass of squarks and drops  $\sim 2$  sec for  $\tilde{m} \sim 10^9$  GeV. If the baryon asymmetry of the universe is generated at a high scale, above  $\sim \tilde{m}/10$ , the requirement that it not be washed out by the  $B$  operator coming into equilibrium at lower temperatures places constraints on  $\lambda_B$ . However, these constraints are relatively weak, since the process is suppressed by the heavy superpartner mass and four-body phase space, and we ignore them here.

The results are very similar for the two lepton number violating RPV operators  $LLe^c$  and  $QLd^c$ . In the first case the Higgsino decays to  $\ell^+ \ell^- \nu$  and the rate is similar to (26) suppressed by  $(m_\tau/m_t)^2$ . In the second case the Higgsino decays to a top quark, a down quark and a charged lepton and the rate is the same as (26).

Bilinear  $R$ -parity violation may also occur through the lepton number violating operator  $\kappa_i L_i H_u$ . This can be generated in a similar way to the  $\mu$  term, of Eq. (12), through a Kähler potential operator of the form  $\frac{W^{\dagger} W^{\dagger}}{\Lambda^3} L H_u$  and so one expects  $\kappa \sim \mu \sim 1$  TeV. This operator leads to two-body Higgsino decays,  $\tilde{H} \rightarrow \ell^\pm W^\mp (\nu Z)$  with a width that scales as,

$$\Gamma_{\tilde{H}} \sim \frac{g^2}{16\pi} \left( \frac{\kappa \Delta}{\mu^2} \right)^2 \mu, \quad (27)$$

where  $\Delta$  is the chargino-neutralino mass splitting, which is  $\sim 340$  MeV. Usually there are strong constraints on the size of  $\kappa_i$  since this operator contributes to neutrinos masses at both tree and loop level [73]. However, for Dirac gauginos the tree-level contributions are suppressed by the Majorana mass of the adjoint partner,  $m_\nu \sim g^2 \langle \tilde{\nu} \rangle^2 M_A / M_D^2$ , which we have taken to be small. Furthermore, the loop-generated masses, that arise through the mixing of Higgsinos with leptons induced by  $\kappa$ , scale as,

$$m_\nu \sim \frac{y_b^4}{16\pi^2} \frac{\kappa^2 v_u v_d}{\mu M_D^4}. \quad (28)$$

Thus,  $\kappa \sim 1$  TeV is allowed by neutrino masses and leads to very fast decays of Higgsinos that are safe cosmologically and can be searched for at colliders.

As mentioned above, the  $\mu$  term is protected by both a PQ- and an  $R$ -symmetry, so one might worry that turning on RPV interactions leads to a new source for generating  $\mu$ . The RGEs in a the general MSSM with RPV are known up to two-loop order [74]. To this order, the running of  $\mu$  is altered from that of the MSSM only if both  $\kappa_i$  and one other source of lepton number violation (i.e.  $LLe^c$  or  $LQD^c$ ) are non-zero, and the effect is proportional to their product. We ignore these effects.

## V. HYPERCHARGE IMPURE MODEL

The pure Dirac model discussed in the previous section, with high scale supersoft supersymmetry breaking, provides an explanation of the Higgs quartic coupling crossing through zero at an intermediate scale (and hence, the correct low energy Higgs mass) combined with gauge coupling unification nontrivially obtained through accelerated running above the intermediate scale. The downside is that the LSP is not a viable dark matter candidate, due to the unsuppressed  $Z$ -exchange with a nearly pure neutral Dirac fermion made up from the two neutral (Majorana) Higgsinos.

We now consider a different model, which we dub the hypercharge impure model, in which the bino does *not* acquire a Dirac mass, and instead obtains the standard one-loop suppressed Majorana contribution from anomaly mediation, Eq. (8). The Majorana bino causes a slight splitting of the pseudo-Dirac neutral Higgsino into two Majorana states. Consequently, the lightest neutral (Majorana) Higgsino can only scatter *inelastically* through  $Z$  exchange [75–77], and thus the spin-independent scattering direct detection rate is suppressed. If the mass splitting  $\gtrsim 200$  keV, there is negligible scattering through  $Z$  exchange due to insufficient kinetic energy to upscatter into the heavier neutral Higgsino state.

<sup>5</sup>The situation does not improve if the Higgsinos are lighter and do not make up all of the dark matter. The lightest Higgsinos can be is  $\sim 100$  GeV (due to the LEP II bound [68]), making them only 1% of the dark matter [10], while the unsuppressed  $Z$ -exchange cross section is roughly six orders of magnitude larger than current direct detection limits.



The absence of a Dirac mass for the bino is automatic if there is no massless singlet for the bino to marry through Eq. (1).<sup>6</sup> By itself this does not directly affect gauge coupling unification. It does, however, have repercussions on the predicted Higgs quartic coupling, and consequently, on the mass scales in the model.

In this model, the wino mass is large ( $\sim M_D$ ), and so the neutralino mixing matrix has the form,

$$\tilde{M}_N = \begin{pmatrix} M_1 & -M_Z c_\beta s_W & M_Z s_\beta s_W \\ -M_Z c_\beta s_W & 0 & -\mu \\ M_Z s_\beta s_W & -\mu & 0 \end{pmatrix}, \quad (29)$$

with  $s_\beta = \sin \beta$ ,  $s_W = \sin \theta_W$  etc. At leading order the lightest two (Majorana) eigenvalues are,

$$\begin{aligned} \tilde{M}_{N1} &= \mu - \frac{M_Z^2 s_W^2}{2M_1} (\sin 2\beta + 1), \\ \tilde{M}_{N2} &= \mu - \frac{M_Z^2 s_W^2}{2M_1} (\sin 2\beta - 1). \end{aligned} \quad (30)$$

The mass difference is independent of  $\mu$  and  $\tan \beta$  and is

$$\Delta \tilde{M}_N = \frac{M_Z^2 \sin^2 \theta_W}{M_1} \simeq (200 \text{ keV}) \frac{10^7 \text{ GeV}}{M_1}. \quad (31)$$

For spin-independent scattering, and for an inelastic splitting exceeding  $\gtrsim 250$  keV, the minimum velocity to scatter with recoil energy  $E_R < 50$  keVnr in xenon is beyond the maximum velocity any WIMP is expected to have (in the Earth's frame) assuming a galactic escape velocity of 550 km/s. There is a loop-induced spin-independent elastic scattering but again, for these large splittings, the rate is much too low to be observed [78,79].<sup>7</sup> At tree level, the lightest chargino, the charged component of the Higgsino, also has mass  $\mu$ . However, there is a loop contribution that splits the charged from the neutral component by  $\sim 340$  MeV [80]. There is also an elastic spin-dependent process, for which the bounds are considerably weaker, but the rate is suppressed since the coupling scales as  $\sim \Delta \tilde{M}_N / \mu$ .

Compared to the pure Dirac model, the spectrum of the squarks, sleptons and Higgs scalars remains relatively unchanged. However, while the pure Dirac model was viable even in the limit of zero  $F$ -term scalar masses, the hypercharge impure model is not. If the only source of supersymmetry breaking is the supersoft operator, Eq. (1),

<sup>6</sup>If the Dirac partners form part of a GUT multiplet, such as a **24**, we imagine that the singlet receives a large mass at the scale where the GUT breaks and is therefore decoupled from physics at  $M_D \ll M_{\text{GUT}}$ .

<sup>7</sup>There is also large destructive interference between the  $W$ -box diagram and Higgs exchange at the curiously enigmatic value of  $m_{\tilde{h}} \simeq 125$  GeV [78].

removing the  $U(1)$  adjoint not only leaves both the bino massless, but the right-handed sleptons as well; they are only charged under  $U(1)_Y$  and would normally receive a mass when the Dirac bino is integrated out. The bino mass is lifted from zero by the anomaly-mediated contribution, however the anomaly-mediated contribution to the right-handed slepton masses is (infamously) tachyonic [58]. Therefore, there must be positive  $F$ -term contributions to the right-handed slepton masses through Eq. (16). To simply the presentation, we assume these contributions are comparable to the one-loop finite contributions to the other scalars from the Dirac gluino and wino.

Since the bino mass in this model is purely Majorana,  $R$ -symmetry is broken and  $\mu$  will be generated radiatively as soon as supersymmetry is broken. The one-loop RG equation for  $\mu$  given in Eq. (14) must be integrated from  $B_\mu$  all the way down to  $M_1$ , a much larger interval than in the pure Dirac case. The larger running interval leads to substantially larger radiative  $\mu$ . Assuming the primordial  $|\mu| \ll |M_1|$ , we obtain

$$\begin{aligned} \mu &\simeq \frac{\tilde{g}_u \tilde{g}'_d}{16\pi^2} M_1^* \ln \frac{|B_\mu|^{1/2}}{|M_1|} \\ &\simeq (1 \text{ TeV}) \sin(2\beta) \frac{M_1^*}{10^6 \text{ GeV}} \ln \frac{|B_\mu|^{1/2}}{|M_1|}. \end{aligned} \quad (32)$$

Depending on  $M_1$  and  $\tan \beta$ , the generated  $\mu$  can easily exceed 1 TeV.

One additional significant consequence follows from the presence of a pure Majorana bino. As shown in Eq. (11),

$$\lambda_h(M_D) = \frac{g^2}{4} \cos^2 2\beta \quad (33)$$

and thus a partial quartic coupling is re-generated. This tends to lower the scale of the Dirac gauginos (and the other derived scales), as we show in more detail in the next subsection.

### A. Gauge coupling unification

We now study gauge coupling unification in this model, again using the weak scale coupling inputs given in Eq. (A2). The RG evolution is done similarly to the pure Dirac model. Choosing a Higgsino mass  $m_{\tilde{H}} \simeq |\mu|$ , we evolve the RG equations from the weak scale up to  $m_{\tilde{H}}$ , and then continue to evolve until the running Higgs quartic coupling  $\lambda_h$  satisfies the boundary condition<sup>8</sup>

$$\lambda_{h,SM+\tilde{H}}(M_D) = \frac{g_{SM+\tilde{H}}^2(M_D)}{4} \cos^2 2\beta. \quad (34)$$

<sup>8</sup>Like the analysis for the pure Dirac model, we assume the contribution from Eq. (6) is negligible.

This sets the Dirac wino mass scale,  $M_D$ , which we take to be the same value for the Dirac gluino. The subscript in the above equation indicates that the  $\lambda_h$  and  $g'$  RGEs contain the effects of all SM fields plus the Higgsinos. This change in the  $\lambda_h$  boundary condition is the major difference between the RG evolution in this model and the pure Dirac model discussed in Sec. IV.

Having established  $M_D$ , we set  $M_1 = fM_D$ , and we consider  $f \in \{10^{-4}, 10^{-3}, 10^{-2}, 10^{-1}\}$ . The range arises from Eq. (9), where  $f \approx 10^{-2}$  is predicted if  $\Lambda = M_{\text{Pl}}$ , the couplings  $\lambda_{2,3} = 1$  in Eq. (1), and the  $D$  term dominates the supersymmetry breaking contributions in the hidden sector. Smaller (or larger) values of  $f$  are easily possible, e.g., when  $\Lambda < M_{\text{Pl}}$  (or when  $\lambda_{2,3} < 1$ ). Generically we expect the squarks and sleptons to be somewhat lighter than  $M_D$ , however for presentation purposes we have set  $\tilde{m} = M_D$  to minimize the number of thresholds we have to deal with. With  $M_1$  and  $M_D$  (and our assumption about  $\tilde{m}$ ), all thresholds are known, and we can complete the RG evolution up to and past these mass scales with suitable matching.

Finally, to check the consistency of our Higgsino mass choice, we also run from UV to IR. Starting at  $M_D$  and assuming  $\mu(M_D) = 0$ , we solve for the radiatively generated  $\mu$ . The choice  $\mu(M_D) = 0$  is somewhat arbitrary, as we have seen that there can be  $O(\text{TeV})$  contributions to  $\mu$  from the higher-dimensional operator shown in Eq. (12). A contribution to  $\mu$  at the scale  $M_D$  is multiplicatively renormalized. For the values of  $M_1$  that we consider, the effect of the multiplicatively renormalized piece of  $\mu$  is

small, however it is possible to arrange for cancellations between this piece and the contribution to  $\mu$  coming from  $M_1$ . Some of this possible parameter space is already incorporated by the large range in  $f = M_1/M_D$ .

The quantities we are interested in for a given set of inputs are: i.) the “quality” of the gauge coupling unification, ii.) the scale of gauge coupling unification, and iii.) the internal consistency of the Higgsino mass.

The quality of unification is a somewhat subjective measure; we choose to calculate the area of the triangle formed, in the usual  $\log(\text{RG scale}) - \alpha^{-1}$  plane, from the three coupling intersection points, i.e., where  $\alpha_3^{-1} = \alpha_1^{-1}$ ,  $\alpha_3^{-1} = \alpha_2^{-1}$ , etc. Each intersection point is a coupling value  $\alpha_{\text{intersect}}^{-1}$  and an energy scale. The area of the triangle is not an ideal measure, since it leads to artificially low values for scenarios that happen to unify at small  $\alpha_{\text{intersect}}^{-1}$ . Therefore, to remove this bias and get a more robust unification measure, we divide the area of the unification triangle divided by the smallest of the three  $\alpha_{\text{intersect}}^{-1}$ . To study how the unification scale changes through parameter space, we keep track of both the lowest and highest energy scales among the intersection points. Finally, we have also calculated the unification measure and range of scales in the MSSM, to directly compare with our model.

The SM input with the greatest impact on the RG evolution and gauge coupling unification is the top mass  $m_t(m_t)$ . A smaller top Yukawa coupling causes the Higgs quartic coupling to evolve more slowly, which in turn postpones the scale where the quartic and gauge couplings

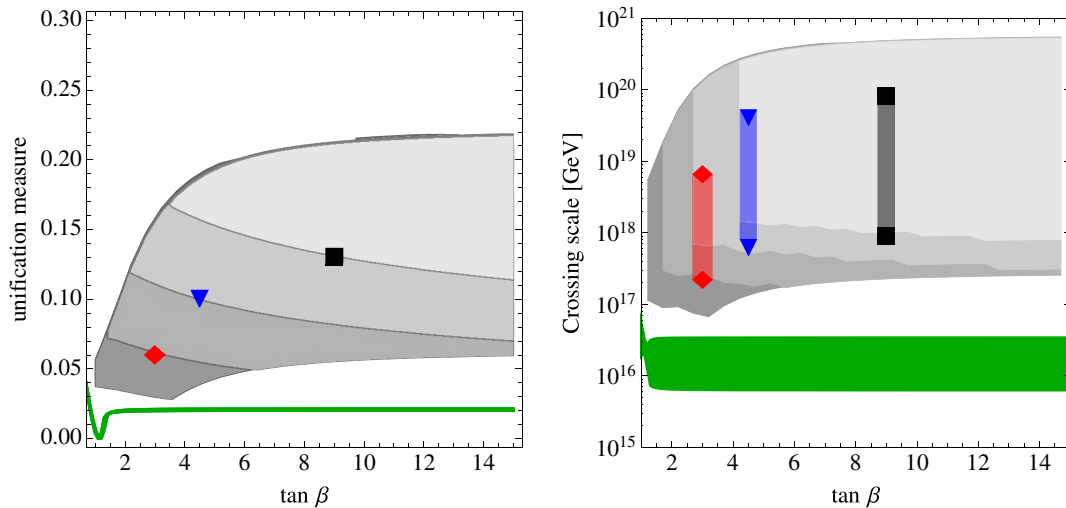


FIG. 3 (color online). The left-side plot shows the unification measure, defined as the area of the triangle formed by the three gauge coupling intersection points, for four different values of  $M_1/M_D$  as  $m_t$  and  $\tan(\beta)$  are varied. The right-side plot shows the gauge coupling unification scale range, defined by the lowest and highest scale where two of the three couplings cross each other. To scale out the dependence of the unification measure on  $\alpha_{\text{intersect}}^{-1}$ , we divide the triangle area by the smallest intersection point value of  $\alpha_{\text{intersect}}^{-1}$ . Only points with consistent Higgsino mass  $\mu < 1.1$  TeV are included in the plot. The contours, reading from upper right to lower left, correspond to  $M_1/M_D = 0.1, 10^{-2}, 10^{-3}$  and  $10^{-4}$ . The smallest (largest)  $m_t$  values correspond to the lowest (highest) edge of each contour. The three markers indicate benchmark  $m_t, \tan(\beta)$  points that we will examine in more detail. To normalize our definition of the unification measure, we show the unification measure assuming the MSSM with all particles at 1 TeV.

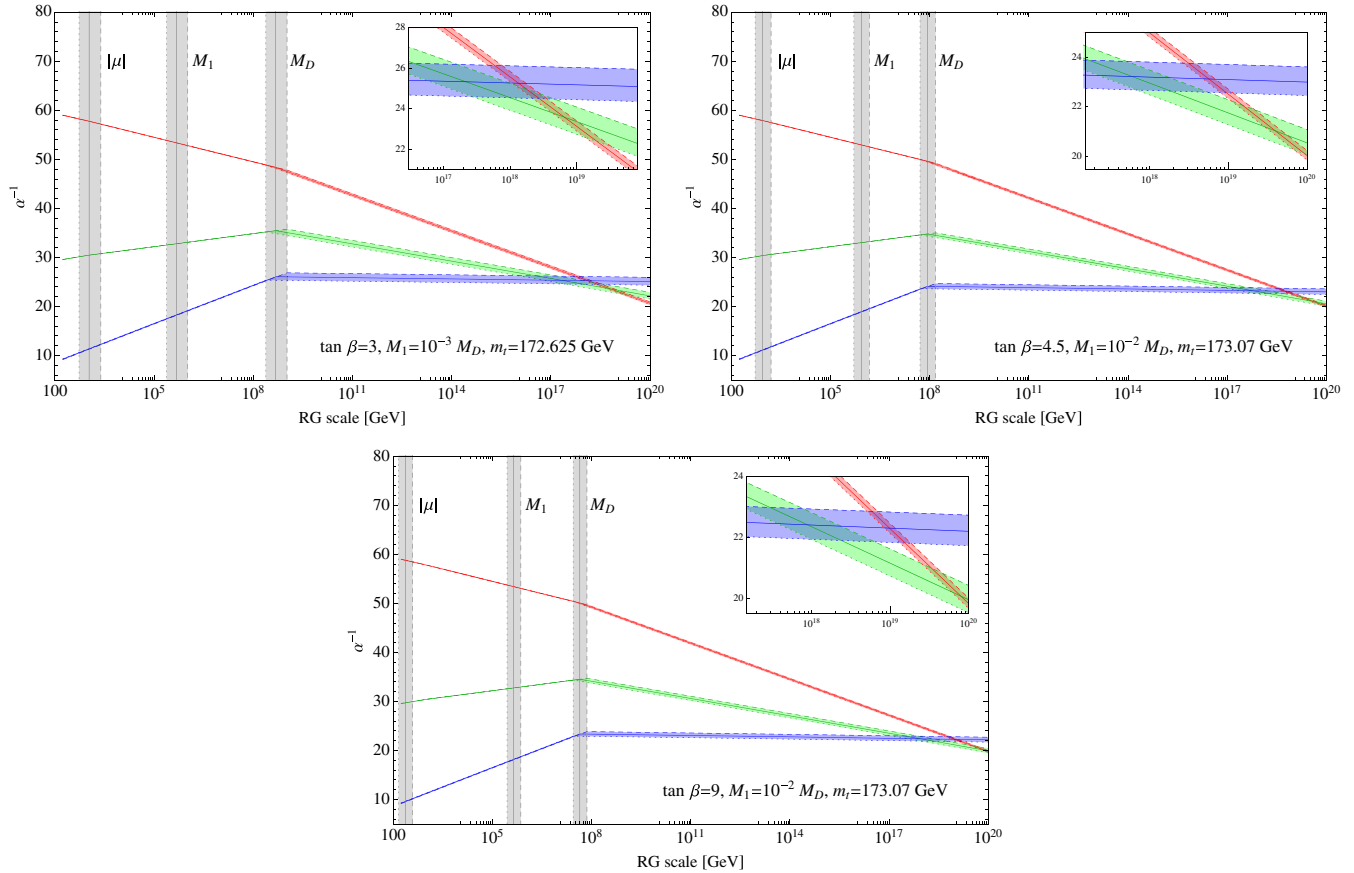


FIG. 4 (color online). The running gauge couplings for the three scenarios indicated by markers in Fig. 3. The top left plot corresponds to the red diamond in Fig. 3, the top right plot corresponds to the blue triangle, and the lower plot corresponds to the black square. In each scenario we show the variation in the unification as the strong coupling  $\alpha_s$  is varied within  $2\sigma$  of its central value. The insets in the upper right of each plot show a zoomed-in picture of the intersection region. As explained in the text, since our procedure for setting  $M_D$  depends on the running of the Higgs quartic, all mass scales, and hence all couplings, shift as  $\alpha_s(M_Z)$  is varied.

intersect, Eq. (34). Conversely, a larger top Yukawa coupling causes the Higgs quartic coupling to evolve faster and tends to lower the mass scales in the theory. We have already seen from the one-loop estimates in Sec. III, as well as the two-loop results shown in Fig. 2, that gauge coupling unification with a Dirac gluino and wino prefers  $M_D \sim 10^{11}$  GeV. Lower  $M_D$  (due to large  $m_t$  values or other effects) causes the gauge coupling unification to be less precise. We account for this dependence by varying  $m_t(m_t)$  within the  $2\sigma$  uncertainty bands in our calculations. The regions formed by varying  $m_t(m_t)$  and  $\tan\beta$  are shown in Fig. 3. As we vary  $m_t(m_t)$  and  $\tan\beta$  we calculate the (one-loop) radiatively generated  $\mu$  term, assuming the primordial  $\mu$  is 0, and keep only those points for which  $\mu \leq 1.1$  TeV. The unification measure and scale in the MSSM (all superpartners at 1 TeV) is also shown in Fig. 3 for comparison.

To give the reader a more concrete context on the quality of gauge coupling unification, we pick three benchmark scenarios to display in more detail. These three benchmark points are indicated by the markers on Fig. 3. From the

$m_t$ ,  $\tan\beta$  and  $M_1/M_D$  inputs corresponding to each point, we show how the gauge couplings evolve with energy, i.e., the analogous plot to Fig. 2. The running couplings for the benchmark points are shown in Fig. 4.

As in Fig. 2, we plot the couplings for three different choices of  $\alpha_s(M_Z)$ . The impact of varying  $\alpha_s(M_Z)$  is larger than one might have expected; all couplings and scales move, some even significantly, as  $\alpha_s(M_Z)$  is varied. This sensitivity comes from the fact that we use the running Higgs quartic, a quantity sensitive to  $\alpha_s(M_Z)$ , to set the location of  $M_D$ . Small changes in  $\alpha_s(M_Z)$  can lead to  $O(1)$  changes in what we derive  $M_D$  to be, and changes in  $M_D$  trickle down to changes in where all running couplings are matched. To better illustrate how the scale  $M_D$  is derived, and how changes in  $\alpha_s(M_Z)$  affect it, we plot the running quartic coupling in each of the benchmark scenarios in Fig. 5 below. Along with  $\lambda_h$ , we also show the running of  $\frac{g^2}{4} \cos^2 2\beta$ , as the intersection of the two curves is what sets  $M_D$ .

We can see from Fig. 3 that, at low  $\tan\beta$  and small  $M_1/M_D$ , unification can be as good as in the MSSM. For

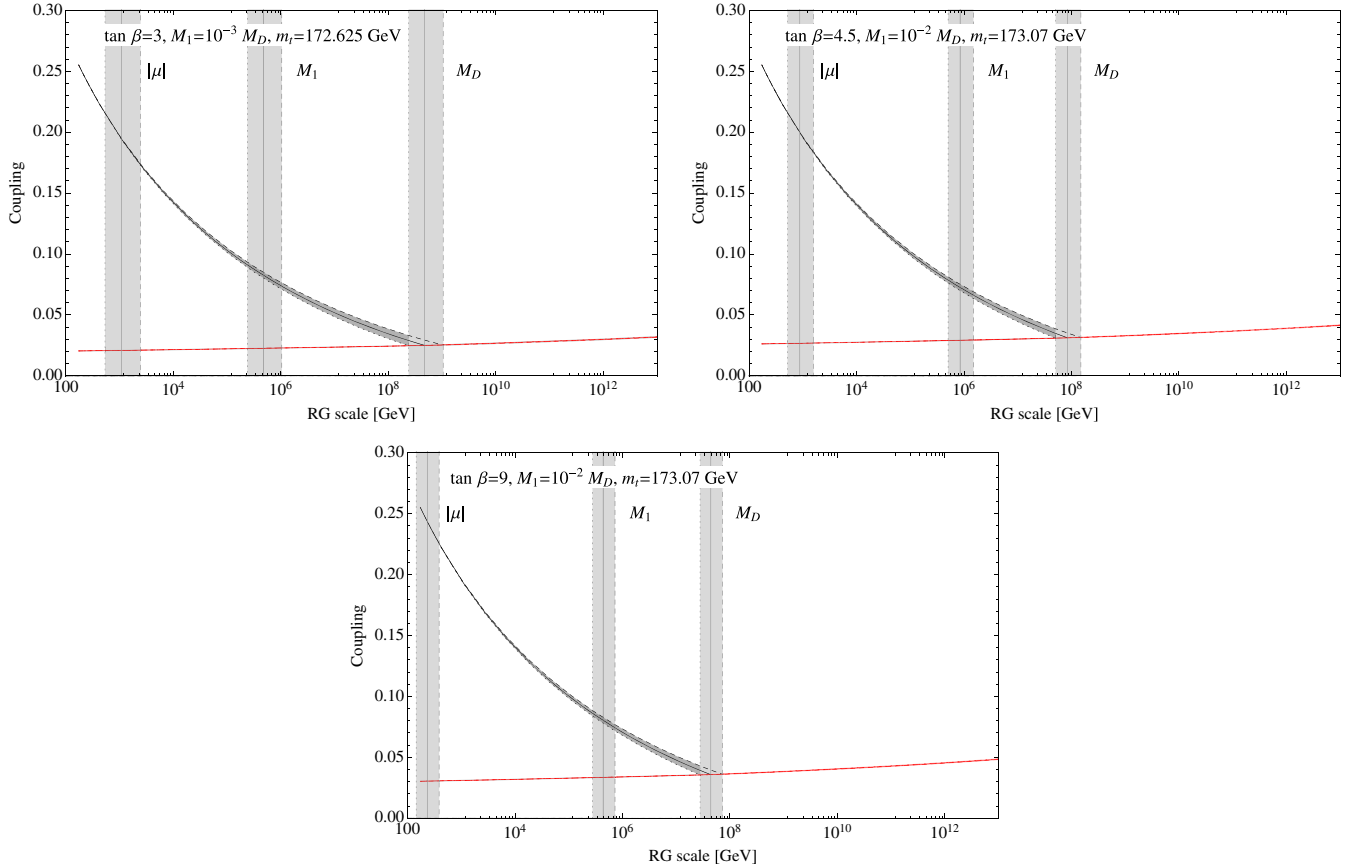


FIG. 5 (color online). The running of the Higgs quartic coupling (black) and  $\frac{g^2}{4} \cos^2 2\beta$  (red) in the three benchmark scenarios indicated on Fig. 3. The layout of scenarios is the same as in Fig. 4.

other parameters, unification is somewhat less precise. The inset plots in Fig. 4 show the mismatch in unification after uncertainties in  $\alpha_s(M_Z)$  are taken into account.

## VI. DISCUSSION

We have presented a new framework for split supersymmetry employing Dirac gaugino masses at intermediate mass scales ( $\sim 10^{8-11}$  GeV). Two specific models were constructed, both containing gauge coupling unification, and one (the hypercharge impure model) with a Higgsino dark matter candidate. There are no model-building gymnastics necessary to suppress  $R$  violation to maintain light gauginos, as in the original split supersymmetry model. The predictivity of split Dirac supersymmetry is improved over simply unnatural/mini-split/spread, see for example Refs. [12,13,60,61,81], in so far as the split superpartner mass scale is determined to be an intermediate scale with a weaker dependence on  $\tan\beta$ .

Both of the discussed models have signals at the weak scale. We emphasize that the signals themselves are qualitatively distinct from other split supersymmetry models—just Higgsinos are light in split Dirac supersymmetry, while binos, winos, gluinos are *heavy*. One of the pressing issues of models that implement the

scalar-to-gaugino mass hierarchy using anomaly mediation [59,82], that can also occur in the Refs. [12,13,60,61,81] and related models [83] is that winolike dark matter is strongly constrained by indirect detection from  $\gamma$ -ray production in the center of the galaxy [84,85], for all DM profiles with a core size smaller than 0.5 kpc. Nearly pure Higgsino-like dark matter, with a mass of  $\approx 1.1$  TeV (which is consistent with thermal abundance), does not suffer from this constraint due to the negligible Sommerfeld enhancement in the annihilation rate. On the contrary, indirect detection may provide one of the promising avenues towards experimental verification [86]. There are several other aspects of split supersymmetry, including flavor physics [87,88] and inflation [89] that could have interesting interpretations in the split Dirac supersymmetry framework.

Another challenge to split supersymmetry models is dimension-five proton decay with anarchic sfermion masses [90,91]. Split Dirac supersymmetry with just  $D$ -term supersymmetry breaking mediation is flavor blind, completely eliminating this issue. Nevertheless, even if anarchic  $F$  terms are also present (and  $F$  terms must be present in the hypercharge impure model), the situation with split Dirac supersymmetry is much improved because of the absence of



Majorana gluinos and winos, and that the only  $R$  violation arises from a one-loop suppressed bino mass that is accompanied by its small  $g'$  couplings to sfermions.

Gauge coupling unification is comparable to the MSSM in the pure Dirac model, and somewhat worse in the hypercharge impure model. Since the predicted unification scale is higher  $\gtrsim 10^{17}$  GeV, the Planck-suppressed GUT threshold corrections are also correspondingly larger. Hence, the slightly less precise unification could be just a symptom of this higher GUT scale. Among the three scales where the gauge couplings intersect,  $\alpha_2 = \alpha_3$  occurs at the lowest scale with  $\alpha_1$  typically  $\sim 5\%$  smaller at this scale. If we take this minor discrepancy as suggestive of low energy physics, this could suggest the sleptons are actually much lighter than the squarks in the model. Such a spectrum is not unexpected since in the hypercharge impure model the source of the (RH) slepton mass is distinct from that for the squarks. There may also be additional fields transforming under  $U(1)_Y$  at low to intermediate scales.

One of the most striking results from our study is the possibility of nearly pure weak scale Higgsino dark matter whose mass  $\mu$  and neutral Higgsino splitting  $\Delta\tilde{M}_N$  arise from the same source—a large Majorana bino mass  $M_1 = 10^6 \rightarrow 10^7$  GeV. Split Dirac supersymmetry (in the hypercharge impure variety) acts as a UV completion of *viable* Higgsino dark matter. Higgsino dark matter produced purely from thermal processes in the early Universe is possible when  $\mu \approx 1.1$  TeV, though lighter Higgsinos are also possible if there is an additional source, e.g., asymmetric Higgsinos [92] or a non-thermal source [93].

There are numerous phenomenological consequences of Higgsino dark matter that warrant a separate study, which we will present in Ref. [86]. On the dark matter side, we would like to know how best to detect an inelastically split Higgsino. Direct detection is highly suppressed, however, there can be a large degree of time and recoil-energy dependence that, to the best of our knowledge, are not being searched for now with existing data. Direct detection through elastic scattering is highly suppressed for both the loop-induced processes leading to spin-independent scattering as well as the tree-level spin-dependent scattering (due to pseudo-Dirac nature of the lightest Higgsino). Indirect detection through  $\gamma$  rays provides a promising detection strategy using proposed future air Cherenkov telescopes [94]. Indirect detection through accumulation and annihilation in the Sun [95–97], white dwarf [98] also provide interesting probes. However, thermalization of dark matter has been *assumed* in Refs. [95,97,98] and unfortunately, the highly suppressed spin-independent elastic scattering suggests thermalization is not effective on timescales of order the age of the solar system. On the collider side, pure Higgsinos are currently unconstrained by the LHC [99], beyond the LEP II bound [68]. Some first studies of Higgsino production at the LHC and at a 100 TeV collider [100] suggest getting to the thermal abundance upper bound

of 1.1 TeV is not trivial. Further studies of nearly degenerate Higgsinos are clearly warranted.

## ACKNOWLEDGMENTS

We thank N. Arkani-Hamed, C. Burgess, P. Saraswat, N. Weiner, and I. Yavin for several useful discussions during the course of the research. G. D. K. thanks L. Hall and Y. Nomura for fun discussions about Ref. [52] prior to that (and this) paper appearing in e-print. G. D. K. is supported in part by the U.S. Department of Energy under Contracts No. DE-FG02-96ER40969 and No. DE-SC0011640. Fermilab is operated by Fermi Research Alliance, LLC, under Contract No. DE-AC02-07CH11359 with the United States Department of Energy.

## APPENDIX A: RG INPUTS

For the RG evolution, we take as boundary conditions [101]

$$\begin{aligned}\alpha_{em}^{-1}(M_Z) &= 127.944 \pm 0.014, \\ \sin^2\theta_W(M_Z) &= 0.23126 \pm 0.00005, \\ \alpha_3(M_Z) &= 0.1185 \pm 0.0006, \\ M_Z(M_Z) &= 91.1876 \pm 0.0021 \text{ GeV}, \\ m_t(m_t) &= 173.07 \pm 0.89 \text{ GeV}, \\ m_h &= 125.9 \pm 0.4 \text{ GeV}.\end{aligned}\tag{A1}$$

## APPENDIX B: RGE IN DIRAC-SPLIT

Here we collect the two-loop renormalization group equations<sup>9</sup> used to evolve couplings from the top mass to the GUT scale, derived using the standard techniques [103–108]. Below the scale  $M_D$ , the superpartner mass scale, we consider the evolution of the Higgs quartic coupling  $\lambda_h$ , the top Yukawa  $y_t$ , and the three gauge couplings  $g_i$ . Above that scale we only evolve the gauge couplings and the top Yukawa. We work in a GUT normalization,  $g_1 = \sqrt{5/3}g_Y$ . It is useful to introduce a general form for the two-loop gauge coupling RGEs,

$$\begin{aligned}\frac{d}{dt}g_i &= \beta_i^{(1)} + \beta_i^{(2)} \\ \kappa\beta_i^{(1)} &= b_i g_i^3 \\ \kappa^2\beta_i^{(2)} &= g_i^3 \left[ \sum_{j=1}^3 B_{ij} g_j^2 - d_i y_t^2 \right],\end{aligned}\tag{B1}$$

where we define the loop factor  $\kappa = 16\pi^2$ . In addition, we define the beta functions

<sup>9</sup>As a check of our method we have derived the 2 loop RGEs for split supersymmetry and agree with the results presented in [102].

$$\frac{d}{dt}y_i = \beta_{y_i}^{(1)} + \beta_{y_i}^{(2)} \quad (\text{B2})$$

$$\frac{d}{dt}\lambda_h = \beta_{\lambda_h}^{(1)} + \beta_{\lambda_h}^{(2)} \quad (\text{B3})$$

with coefficients as given below.

### 1. Standard Model

Above the top quark mass, but below the Higgsino mass, the field content is identical to the SM. Thus,

$$b = \left(\frac{41}{10}, -\frac{19}{6}, -7\right), \quad B = \begin{pmatrix} \frac{199}{50} & \frac{27}{10} & \frac{44}{5} \\ \frac{9}{10} & \frac{35}{6} & 12 \\ \frac{11}{10} & \frac{9}{2} & -26 \end{pmatrix},$$

$$d = \left(\frac{17}{10}, \frac{3}{2}, 2\right). \quad (\text{B4})$$

Similarly the running of the Yukawa and quartic are as in the SM,

$$\kappa\beta_{y_i}^{(1)} = \frac{9}{2}y_i^3 - y_i\left(8g_3^2 + \frac{9}{4}g_2^2 + \frac{17}{20}g_1^2\right) \quad (\text{B5})$$

$$\begin{aligned} \kappa^2\beta_{y_i}^{(2)} = & -12y_i^5 + y_i^3\left(36g_3^2 + \frac{225}{16}g_2^2 + \frac{393}{80}g_1^2 - 6\lambda_h\right) \\ & + y_i\left(-108g_3^4 + 9g_2^2g_3^2 + \frac{19}{15}g_3^2g_1^2 - \frac{23}{4}g_2^4\right. \\ & \left. - \frac{9}{20}g_2^2g_1^2 + \frac{1187}{600}g_1^4 + \frac{3}{2}\lambda_h^2\right), \end{aligned} \quad (\text{B6})$$

and

$$\begin{aligned} \kappa\beta_{\lambda_h}^{(1)} = & 12\lambda_h^2 + \lambda_h\left(12y_t^2 - 9g_2^2 - \frac{9}{5}g_1^2\right) \\ & - 12y_t^4 + \frac{9}{4}g_2^4 + \frac{9}{10}g_2^2g_1^2 + \frac{27}{100}g_1^4 \end{aligned} \quad (\text{B7})$$

$$\begin{aligned} \kappa^2\beta_{\lambda_h}^{(2)} = & -78\lambda_h^3 + \lambda_h^2\left(54g_2^2 + \frac{54}{5}g_1^2 - 72y_t^2\right) \\ & + \lambda_h\left(-3y_t^4 + y_t^2\left(80g_3^2 + \frac{45}{2}g_2^2 + \frac{17}{2}g_1^2\right)\right. \\ & \left. - \frac{73}{8}g_2^4 + \frac{117}{20}g_2^2g_1^2 + \frac{1887}{200}g_1^4\right) \\ & + 60y_t^6 - y_t^4\left(64g_3^2 + \frac{16}{5}g_1^2\right) \\ & + y_t^2\left(-\frac{9}{2}g_2^4 + \frac{63}{5}g_2^2g_1^2 - \frac{171}{50}g_1^4\right) + \frac{305}{8}g_2^6 \\ & - \frac{289}{40}g_2^4g_1^2 - \frac{1677}{200}g_2^2g_1^4 - \frac{3411}{1000}g_1^6. \end{aligned} \quad (\text{B8})$$

### 2. The Standard Model with Higgsinos

The inclusion of the vectorlike Higgsinos alters the running of the gauge couplings at one loop, and the quartic and top Yukawa at two loops. Thus,

$$b = \left(\frac{9}{2}, -\frac{5}{2}, -7\right) \quad B = \begin{pmatrix} \frac{104}{25} & \frac{18}{5} & \frac{44}{5} \\ \frac{6}{5} & 14 & 12 \\ \frac{11}{10} & \frac{9}{2} & -26 \end{pmatrix}$$

$$d = \left(\frac{17}{10}, \frac{3}{2}, 2\right). \quad (\text{B9})$$

Since the one-loop running is as in the SM we only show the two-loop contributions. First for the top Yukawa,

$$\begin{aligned} \kappa^2\beta_{y_t}^{(2)} = & -12y_t^5 + y_t^3\left(36g_3^2 + \frac{225}{16}g_2^2 + \frac{393}{80}g_1^2 - 6\lambda_h\right) \\ & + y_t\left(-108g_3^4 + 9g_2^2g_3^2 + \frac{19}{15}g_3^2g_1^2 - \frac{21}{4}g_2^4\right. \\ & \left. - \frac{9}{20}g_2^2g_1^2 + \frac{1303}{600}g_1^4 + \frac{3}{2}\lambda_h^2\right). \end{aligned} \quad (\text{B10})$$

Then the Higgs quartic coupling,

$$\begin{aligned} \kappa^2\beta_{\lambda_h}^{(2)} = & -78\lambda_h^3 + \lambda_h^2\left(54g_2^2 + \frac{54}{5}g_1^2 - 72y_t^2\right) \\ & + \lambda_h\left(-3y_t^4 + y_t^2\left(80g_3^2 + \frac{45}{2}g_2^2 + \frac{17}{2}g_1^2\right)\right. \\ & \left. - \frac{33}{8}g_2^4 + \frac{117}{20}g_2^2g_1^2 + \frac{2007}{200}g_1^4\right) + 60y_t^6 \\ & - y_t^4\left(64g_3^2 + \frac{16}{5}g_1^2\right) \\ & + y_t^2\left(-\frac{9}{2}g_2^4 + \frac{63}{5}g_2^2g_1^2 - \frac{171}{50}g_1^4\right) + \frac{273}{8}g_2^6 \\ & - \frac{321}{40}g_2^4g_1^2 - \frac{1773}{200}g_2^2g_1^4 - \frac{3699}{1000}g_1^6. \end{aligned} \quad (\text{B11})$$

### 3. The Standard Model with Higgsinos and a Bino

In the second version of the model the bino does not have an adjoint partner to marry and is considerably lighter than the other superpartners. While the addition of a pure gauge singlet does not alter the running of the gauge couplings directly, the presence of both the Higgsinos and bino as propagating degrees of freedom means there are additional Yukawa couplings we have to consider,

$$\mathcal{L} \supset \frac{\tilde{g}'_u}{\sqrt{2}}H^\dagger\tilde{B}\tilde{H}_u + \frac{\tilde{g}'_d}{\sqrt{2}}(H^T e)\tilde{B}\tilde{H}_d + \text{H.c.} \quad (\text{B12})$$

These interactions are the supersymmetrization of the  $U(1)_Y$  gauge-matter interactions. Had both Higgses been

as light as the bino, this piece would have been combined into the supersymmetric  $O(g^5)$  piece of the RGE. However, since only one Higgs is (tuned to be) light, the Higgsino-Higgs-bino interactions is instead projected onto that light

combination, matched at the bino mass, then run as Yukawa couplings. Matching at this scale  $\tilde{g}'_u = g' \sin \beta$ ,  $\tilde{g}'_d = g' \cos \beta$ . These additional Yukawa interactions alter the two-loop gauge RGE, (B1) is modified to become,

$$\kappa^2 \frac{d}{dt} g_i = \kappa b_i g_i^3 + \frac{g_i^3}{(4\pi)^2} \left[ \sum_{j=1}^3 B_{ij} g_j^2 - d_i y_i^2 - d_{B,i} (\tilde{g}'_u{}^2 + \tilde{g}'_d{}^2) \right], \quad (\text{B13})$$

Since we have only added a gauge singlet the  $b, B$  and  $d$  coefficients are unaltered. The new coefficient is,

$$d_B = \left( \frac{3}{20}, \frac{1}{4}, 0 \right). \quad (\text{B14})$$

In turn these new couplings have their own RGEs,

$$\kappa \beta_{\tilde{g}'_u}^{(1)} = \frac{5}{4} \tilde{g}'_u{}^3 + \tilde{g}'_u \left( 2\tilde{g}'_d{}^2 + 3y_t^2 - \left( \frac{9}{4} g_2^2 + \frac{9}{20} g_1^2 \right) \right), \quad (\text{B15})$$

$$\begin{aligned} \kappa^2 \beta_{\tilde{g}'_u}^{(2)} = & -\frac{3}{4} \tilde{g}'_u{}^5 + \tilde{g}'_u{}^3 \left( -\frac{27}{8} y_t^2 + \frac{165}{32} g_2^2 + \frac{309}{160} g_1^2 - 3\lambda_h - \frac{15}{4} \tilde{g}'_d{}^2 \right) + \tilde{g}'_u \left( -\frac{27}{4} y_t^4 + y_t^2 \left( 20g_3^2 + \frac{17}{8} g_1^2 + \frac{45}{8} g_2^2 \right) \right. \\ & \left. - \frac{21}{4} g_2^4 - \frac{27}{20} g_2^2 g_1^2 + \frac{117}{200} g_1^4 + \frac{3}{2} \lambda_h^2 + \tilde{g}'_d{}^2 \left( \frac{39}{8} g_2^2 + \frac{3}{40} g_1^2 - 3\lambda_h \right) - \frac{21}{4} \tilde{g}'_d{}^2 y_t^2 - \frac{9}{4} \tilde{g}'_d{}^4 \right), \end{aligned} \quad (\text{B16})$$

and

$$\kappa \beta_{\tilde{g}'_d}^{(1)} = \frac{5}{4} \tilde{g}'_d{}^3 + \tilde{g}'_d \left( 2\tilde{g}'_u{}^2 + 3y_t^2 - \left( \frac{9}{4} g_2^2 + \frac{9}{20} g_1^2 \right) \right), \quad (\text{B17})$$

$$\begin{aligned} \kappa^2 \beta_{\tilde{g}'_d}^{(2)} = & -\frac{3}{4} \tilde{g}'_d{}^5 + \tilde{g}'_d{}^3 \left( -\frac{27}{8} y_t^2 + \frac{165}{32} g_2^2 + \frac{309}{160} g_1^2 - 3\lambda_h - \frac{15}{4} \tilde{g}'_u{}^2 \right) + \tilde{g}'_d \left( -\frac{27}{4} y_t^4 + y_t^2 \left( 20g_3^2 + \frac{17}{8} g_1^2 + \frac{45}{8} g_2^2 \right) \right. \\ & \left. - \frac{21}{4} g_2^4 - \frac{27}{20} g_2^2 g_1^2 + \frac{117}{200} g_1^4 + \frac{3}{2} \lambda_h^2 + \tilde{g}'_u{}^2 \left( \frac{39}{8} g_2^2 + \frac{3}{40} g_1^2 - 3\lambda_h \right) - \frac{21}{4} \tilde{g}'_u{}^2 y_t^2 - \frac{9}{4} \tilde{g}'_u{}^4 \right). \end{aligned} \quad (\text{B18})$$

These new couplings also enter in the running of the quartic and the top Yukawa. These top Yukawa RGE is given by,

$$\kappa \beta_{y_t}^{(1)} = \frac{9}{2} y_t^3 + y_t \left( \frac{1}{2} \tilde{g}'_u{}^2 + \frac{1}{2} \tilde{g}'_d{}^2 - \left( 8g_3^2 + \frac{9}{4} g_2^2 + \frac{17}{20} g_1^2 \right) \right), \quad (\text{B19})$$

$$\begin{aligned} \kappa^2 \beta_{y_t}^{(2)} = & -12y_t^5 + y_t^3 \left( 36g_3^2 + \frac{225}{16} g_2^2 + \frac{393}{80} g_1^2 - 6\lambda_h - \frac{9}{8} (\tilde{g}'_u{}^2 + \tilde{g}'_d{}^2) \right) \\ & + y_t \left( -108g_3^4 + 9g_3^2 g_2^2 + \frac{19}{15} g_3^2 g_1^2 - \frac{21}{4} g_2^4 - \frac{9}{20} g_2^2 g_1^2 + \frac{1303}{600} g_1^4 + \frac{3}{2} \lambda_h^2 + \left( \frac{15}{16} g_2^2 + \frac{3}{16} g_1^2 \right) (\tilde{g}'_u{}^2 + \tilde{g}'_d{}^2) \right. \\ & \left. - \frac{9}{16} (\tilde{g}'_u{}^4 + \tilde{g}'_d{}^4) - \frac{5}{4} \tilde{g}'_u{}^2 \tilde{g}'_d{}^2 \right). \end{aligned} \quad (\text{B20})$$

The quartic RGE is,

$$\kappa \beta_{\lambda_h}^{(1)} = 12\lambda_h^2 + \lambda_h \left( 12y_t^2 - 9g_2^2 - \frac{9}{5} g_1^2 + 2(\tilde{g}'_u{}^2 + \tilde{g}'_d{}^2) \right) - 12y_t^4 + \frac{9}{4} g_2^4 + \frac{9}{10} g_2^2 g_1^2 + \frac{27}{100} g_1^4 - (\tilde{g}'_u{}^2 + \tilde{g}'_d{}^2)^2, \quad (\text{B21})$$

$$\begin{aligned}
\kappa^2 \beta_{\lambda_h}^{(2)} = & -78\lambda_h^3 + \lambda_h^2 \left( 54g_2^2 + \frac{54}{5}g_1^2 - 72y_t^2 - 12(\tilde{g}_u'^2 + \tilde{g}_d'^2) \right) + \lambda_h \left( -3y_t^4 + 80g_3^2y_t^2 + \frac{45}{2}g_2^2y_t^2 + \frac{17}{2}g_1^2y_t^2 - \frac{33}{8}g_2^4 \right. \\
& + \frac{117}{20}g_2^2g_1^2 + \frac{2007}{200}g_1^4 + \left( \frac{15}{4}g_2^2 + \frac{3}{4}g_1^2 \right) (\tilde{g}_d'^2 + \tilde{g}_u'^2) - \frac{1}{4}\tilde{g}_u'^4 - \frac{1}{4}\tilde{g}_d'^4 + 3\tilde{g}_u'^2\tilde{g}_d'^2 \left. \right) + 60y_t^6 - y_t^4 \left( 64g_3^2 + \frac{16}{5}g_1^2 \right) \\
& + y_t^2 \left( -\frac{9}{2}g_2^4 + \frac{63}{5}g_2^2g_1^2 - \frac{171}{50}g_1^4 \right) + \frac{273}{8}g_2^6 - \frac{321}{40}g_2^4g_1^2 - \frac{1773}{200}g_2^2g_1^4 - \frac{3699}{1000}g_1^6 \\
& - \left( \frac{3}{4}g_2^4 + \frac{3}{10}g_2^2g_1^2 + \frac{9}{100}g_1^4 \right) (\tilde{g}_u'^2 + \tilde{g}_d'^2) + \frac{5}{2}(\tilde{g}_u'^6 + \tilde{g}_d'^6) + \frac{17}{2}\tilde{g}_u'^2\tilde{g}_d'^2(\tilde{g}_u'^2 + \tilde{g}_d'^2). \tag{B22}
\end{aligned}$$

#### 4. The MSSM with Adjoins

The final epoch we are interested in occurs in both Model I and II once all the superpartners, the second Higgs doublet, and the adjoint chiral super fields are included. The field content is that of the MSSM with additional adjoint fermions and scalars. As the adjoints have no supersymmetric interactions outside of the kinetic term, no new couplings are introduced and all  $O(g^3y^2)$  pieces of the gauge couplings RGEs are the same as in the MSSM. Namely the coefficients in (B1) are,

$$\begin{aligned}
b = \left( \frac{33}{5}, 3, 0 \right) \quad B = \begin{pmatrix} \frac{199}{25} & \frac{27}{5} & \frac{88}{5} \\ \frac{9}{5} & 49 & 24 \\ \frac{11}{5} & 9 & 68 \end{pmatrix} \\
d = \left( \frac{26}{5}, 6, 4 \right). \tag{B23}
\end{aligned}$$

Since we are now in a supersymmetric theory the Higgs quartic is no longer a separate coupling but is instead determined from the  $D$  terms in terms of gauge couplings. This leaves only the top Yukawa, which runs as

$$\kappa \beta_{y_t}^{(1)} = 6y_t^3 - y_t \left( \frac{16}{3}g_3^2 + 3g_2^2 + \frac{13}{15}g_1^2 \right) \tag{B24}$$

$$\begin{aligned}
\kappa^2 \beta_{y_t}^{(2)} = & -22y_t^5 + y_t^3 \left( 16g_3^2 + 6g_2^2 + \frac{6}{5}g_1^2 \right) \\
& + y_t \left( -\frac{16}{9}g_3^4 + 8g_2^2g_3^2 + \frac{136}{45}g_1^2g_3^2 + \frac{15}{2}g_2^4 \right. \\
& \left. + g_1^2g_2^2 + \frac{2743}{450}g_1^4 \right). \tag{B25}
\end{aligned}$$

- 
- [1] G. Aad *et al.* (ATLAS Collaboration), *Phys. Lett. B* **716**, 1 (2012).
  - [2] S. Chatrchyan *et al.* (CMS Collaboration), *Phys. Lett. B* **716**, 30 (2012).
  - [3] A. Arbey, M. Battaglia, A. Djouadi, F. Mahmoudi, and J. Quevillon, *Phys. Lett. B* **708**, 162 (2012).
  - [4] P. Draper, P. Meade, M. Reece, and D. Shih, *Phys. Rev. D* **85**, 095007 (2012).
  - [5] A. Delgado, G. F. Giudice, G. Isidori, M. Pierini, and A. Strumia, *Eur. Phys. J. C* **73**, 2370 (2013).
  - [6] J. L. Feng, P. Kant, S. Profumo, and D. Sanford, *Phys. Rev. Lett.* **111**, 131802 (2013).
  - [7] P. Draper, G. Lee, and C. E. M. Wagner, *Phys. Rev. D* **89**, 055023 (2014).
  - [8] N. Arkani-Hamed and S. Dimopoulos, *J. High Energy Phys.* **06** (2005) 073.
  - [9] A. Arvanitaki, C. Davis, P. W. Graham, and J. G. Wacker, *Phys. Rev. D* **70**, 117703 (2004).
  - [10] G. F. Giudice and A. Romanino, *Nucl. Phys.* **B699**, 65 (2004); **B706**, 487(E) (2005).
  - [11] G. F. Giudice and A. Strumia, *Nucl. Phys.* **B858**, 63 (2012).
  - [12] L. J. Hall and Y. Nomura, *J. High Energy Phys.* **01** (2012) 082.
  - [13] N. Arkani-Hamed, A. Gupta, D. E. Kaplan, N. Weiner, and T. Zorawski, [arXiv:1212.6971](https://arxiv.org/abs/1212.6971).
  - [14] M. Ibe, S. Matsumoto, and T. T. Yanagida, *Phys. Lett. B* **732**, 214 (2014).
  - [15] P. Fayet, *Phys. Lett.* **78B**, 417 (1978).
  - [16] J. Polchinski and L. Susskind, *Phys. Rev. D* **26**, 3661 (1982).
  - [17] L. J. Hall and L. Randall, *Nucl. Phys.* **B352**, 289 (1991).
  - [18] P. J. Fox, A. E. Nelson, and N. Weiner, *J. High Energy Phys.* **08** (2002) 035.
  - [19] A. E. Nelson, N. Rius, V. Sanz, and M. Unsal, *J. High Energy Phys.* **08** (2002) 039.
  - [20] Z. Chacko, P. J. Fox, and H. Murayama, *Nucl. Phys.* **B706**, 53 (2005).
  - [21] L. M. Carpenter, P. J. Fox, and D. E. Kaplan, [arXiv:hep-ph/0503093](https://arxiv.org/abs/hep-ph/0503093).



- [22] I. Antoniadis, A. Delgado, K. Benakli, M. Quiros, and M. Tuckmantel, *Phys. Lett. B* **634**, 302 (2006).
- [23] Y. Nomura, D. Poland, and B. Tweedie, *Nucl. Phys.* **B745**, 29 (2006).
- [24] I. Antoniadis, K. Benakli, A. Delgado, and M. Quiros, *Adv. Stud. Theor. Phys.* **2**, 645 (2008).
- [25] G. D. Kribs, E. Poppitz, and N. Weiner, *Phys. Rev. D* **78**, 055010 (2008).
- [26] S. D. L. Amigo, A. E. Blechman, P. J. Fox, and E. Poppitz, *J. High Energy Phys.* **01** (2009) 018.
- [27] K. Benakli and M. D. Goodsell, *Nucl. Phys.* **B816**, 185 (2009).
- [28] K. Benakli and M. D. Goodsell, *Nucl. Phys.* **B830**, 315 (2010).
- [29] K. Benakli and M. D. Goodsell, *Nucl. Phys.* **B840**, 1 (2010).
- [30] G. D. Kribs, T. Okui, and T. S. Roy, *Phys. Rev. D* **82**, 115010 (2010).
- [31] S. Abel and M. Goodsell, *J. High Energy Phys.* **06** (2011) 064.
- [32] R. Davies, J. March-Russell, and M. McCullough, *J. High Energy Phys.* **04** (2011) 108.
- [33] K. Benakli, M. D. Goodsell, and A.-K. Maier, *Nucl. Phys.* **B851**, 445 (2011).
- [34] P. Kumar and E. Ponton, *J. High Energy Phys.* **11** (2011) 037.
- [35] C. Frugiuele and T. Gregoire, *Phys. Rev. D* **85**, 015016 (2012).
- [36] H. Itoyama and N. Maru, *Int. J. Mod. Phys. A* **27**, 1250159 (2012).
- [37] C. Frugiuele, T. Gregoire, P. Kumar, and E. Ponton, *J. High Energy Phys.* **03** (2013) 156.
- [38] J. A. Casas, J. R. Espinosa, and M. Quiros, *Phys. Lett. B* **342**, 171 (1995).
- [39] J. A. Casas, J. R. Espinosa, and M. Quiros, *Phys. Lett. B* **382**, 374 (1996).
- [40] G. Isidori, G. Ridolfi, and A. Strumia, *Nucl. Phys.* **B609**, 387 (2001).
- [41] J. Ellis, J. R. Espinosa, G. F. Giudice, A. Hoecker, and A. Riotto, *Phys. Lett. B* **679**, 369 (2009).
- [42] J. Elias-Miro, J. R. Espinosa, G. F. Giudice, G. Isidori, A. Riotto, and A. Strumia, *Phys. Lett. B* **709**, 222 (2012).
- [43] F. Bezrukov, M. Y. Kalmykov, B. A. Kniehl, and M. Shaposhnikov, *J. High Energy Phys.* **10** (2012) 140.
- [44] G. Degrassi, S. Di Vita, J. Elias-Miro, J. R. Espinosa, G. F. Giudice, G. Isidori, and A. Strumia, *J. High Energy Phys.* **08** (2012) 098.
- [45] D. Buttazzo, G. Degrassi, P. P. Giardino, G. F. Giudice, F. Sala, A. Salvio, and A. Strumia, *J. High Energy Phys.* **12** (2013) 089.
- [46] A. Hebecker, A. K. Knochel, and T. Weigand, *J. High Energy Phys.* **06** (2012) 093.
- [47] G. F. Giudice, R. Rattazzi, and A. Strumia, *Phys. Lett. B* **715**, 142 (2012).
- [48] L. E. Ibanez, F. Marchesano, D. Regalado, and I. Valenzuela, *J. High Energy Phys.* **07** (2012) 195.
- [49] J. Unwin, *Phys. Rev. D* **86**, 095002 (2012).
- [50] L. E. Ibanez and I. Valenzuela, *J. High Energy Phys.* **05** (2013) 064.
- [51] A. Hebecker, A. K. Knochel, and T. Weigand, *Nucl. Phys.* **B874**, 1 (2013).
- [52] L. J. Hall and Y. Nomura, *J. High Energy Phys.* **02** (2014) 129.
- [53] L. J. Hall, Y. Nomura, and S. Shirai, *J. High Energy Phys.* **06** (2014) 137.
- [54] N. Arkani-Hamed, S. Dimopoulos, and S. Kachru, *arXiv: hep-th/0501082*.
- [55] R. Mahbubani and L. Senatore, *Phys. Rev. D* **73**, 043510 (2006).
- [56] M. Dine, A. E. Nelson, Y. Nir, and Y. Shirman, *Phys. Rev. D* **53**, 2658 (1996).
- [57] C. Csaki, J. Goodman, R. Pavesi, and Y. Shirman, *Phys. Rev. D* **89**, 055005 (2014).
- [58] L. Randall and R. Sundrum, *Nucl. Phys.* **B557**, 79 (1999).
- [59] G. F. Giudice, M. A. Luty, H. Murayama, and R. Rattazzi, *J. High Energy Phys.* **12** (1998) 027.
- [60] M. Ibe, S. Matsumoto, and T. T. Yanagida, *Phys. Rev. D* **85**, 095011 (2012).
- [61] A. Arvanitaki, N. Craig, S. Dimopoulos, and G. Villadoro, *J. High Energy Phys.* **02** (2013) 126.
- [62] D. J. Broadhurst, N. Gray, and K. Schilcher, *Z. Phys. C* **52**, 111 (1991).
- [63] K. Melnikov and T. v. Ritbergen, *Phys. Lett. B* **482**, 99 (2000).
- [64] K. G. Chetyrkin and M. Steinhauser, *Nucl. Phys.* **B573**, 617 (2000).
- [65] R. Hempfling and B. A. Kniehl, *Phys. Rev. D* **51**, 1386 (1995).
- [66] F. Jegerlehner and M. Y. Kalmykov, *Nucl. Phys.* **B676**, 365 (2004).
- [67] N. Arkani-Hamed, A. Delgado, and G. F. Giudice, *Nucl. Phys.* **B741**, 108 (2006).
- [68] [http://lepsusy.web.cern.ch/lepsusy/www/inoslowdmsummer02/charginowdm\\_pub.html](http://lepsusy.web.cern.ch/lepsusy/www/inoslowdmsummer02/charginowdm_pub.html).
- [69] M. Kawasaki, K. Kohri, and T. Moroi, *Phys. Rev. D* **71**, 083502 (2005).
- [70] M. Kawasaki, K. Kohri, and T. Moroi, *Phys. Lett. B* **625**, 7 (2005).
- [71] K. Jedamzik, *Phys. Rev. D* **74**, 103509 (2006).
- [72] K. Jedamzik and M. Pospelov, *New J. Phys.* **11**, 105028 (2009).
- [73] L. J. Hall and M. Suzuki, *Nucl. Phys.* **B231**, 419 (1984).
- [74] B. C. Allanach, A. Dedes, and H. K. Dreiner, *Phys. Rev. D* **60**, 056002 (1999); **86**, 039906(E) (2012).
- [75] D. Tucker-Smith and N. Weiner, *Phys. Rev. D* **64**, 043502 (2001).
- [76] D. Tucker-Smith and N. Weiner, *Phys. Rev. D* **72**, 063509 (2005).
- [77] S. Chang, G. D. Kribs, D. Tucker-Smith, and N. Weiner, *Phys. Rev. D* **79**, 043513 (2009).
- [78] R. J. Hill and M. P. Solon, *Phys. Rev. Lett.* **112**, 211602 (2014).
- [79] R. J. Hill and M. P. Solon, *arXiv:1401.3339*.
- [80] M. Cirelli, N. Fornengo, and A. Strumia, *Nucl. Phys.* **B753**, 178 (2006).
- [81] L. J. Hall, Y. Nomura, and S. Shirai, *J. High Energy Phys.* **01** (2013) 036.
- [82] J. D. Wells, *Phys. Rev. D* **71**, 015013 (2005).
- [83] K. Cheung and C. -W. Chiang, *Phys. Rev. D* **71**, 095003 (2005).

- [84] T. Cohen, M. Lisanti, A. Pierce, and T.R. Slatyer, *J. Cosmol. Astropart. Phys.* **10** (2013) 061.
- [85] J. Fan and M. Reece, *J. High Energy Phys.* **10** (2013) 124.
- [86] P.J. Fox, G. D. Kribs, and A. Martin (to be published).
- [87] W. Altmannshofer, R. Harnik, and J. Zupan, *J. High Energy Phys.* **11** (2013) 202.
- [88] M. Baumgart, D. Stolarski, and T. Zorawski, *Phys. Rev. D* **90**, 055001 (2014).
- [89] N. Craig and D. Green, *J. High Energy Phys.* **07** (2014) 102.
- [90] M. Dine, P. Draper, and W. Shepherd, *J. High Energy Phys.* **02** (2014) 027.
- [91] N. Nagata and S. Shirai, *J. High Energy Phys.* **03** (2014) 049.
- [92] K. Blum, A. Efrati, Y. Grossman, Y. Nir, and A. Riotto, *Phys. Rev. Lett.* **109**, 051302 (2012).
- [93] R. Allahverdi, B. Dutta, and K. Sinha, *Phys. Rev. D* **86**, 095016 (2012).
- [94] M. Actis *et al.* (CTA Collaboration), *Exp. Astron.* **32**, 193 (2011).
- [95] A. Menon, R. Morris, A. Pierce, and N. Weiner, *Phys. Rev. D* **82**, 015011 (2010).
- [96] S. Nussinov, L.-T. Wang, and I. Yavin, *J. Cosmol. Astropart. Phys.* **08** (2009) 037.
- [97] J. Shu, P.-f. Yin, and S.-h. Zhu, *Phys. Rev. D* **81**, 123519 (2010).
- [98] M. McCullough and M. Fairbairn, *Phys. Rev. D* **81**, 083520 (2010).
- [99] Z. Han, G. D. Kribs, A. Martin, and A. Menon, *Phys. Rev. D* **89**, 075007 (2014).
- [100] M. Low and L.-T. Wang, *J. High Energy Phys.* **08** (2014) 161.
- [101] J. Beringer *et al.* (Particle Data Group), *Phys. Rev. D* **86**, 010001 (2012) and 2013 partial update for the 2014 edition.
- [102] M. Binger, *Phys. Rev. D* **73**, 095001 (2006).
- [103] M. E. Machacek and M. T. Vaughn, *Nucl. Phys.* **B222**, 83 (1983).
- [104] M. E. Machacek and M. T. Vaughn, *Nucl. Phys.* **B236**, 221 (1984).
- [105] M. E. Machacek and M. T. Vaughn, *Nucl. Phys.* **249B**, 70 (1985).
- [106] S. P. Martin and M. T. Vaughn, *Phys. Rev. D* **50**, 2282 (1994); S. P. Martin and M. T. Vaughn *Phys. Rev. D* **78**, 039903(E) (2008).
- [107] M.-x. Luo, H.-w. Wang, and Y. Xiao, *Phys. Rev. D* **67**, 065019 (2003).
- [108] M. D. Goodsell, *J. High Energy Phys.* **01** (2013) 066.